Nitrogen oxides and ozone fluxes from an oilseed-rape management cycle: the influence of cattle slurry application

Raffaella M. Vuolo[1], Benjamin Loubet[1*], Nicolas Mascher[1], Jean-Christophe Gueudet[1], Brigitte Durand[1], Patricia Laville[1], Olivier Zurfluh[1], Raluca Ciuraru[1], Patrick Stella[2] and Ivonne Trebs[3]

1 UMR ECOSYS, INRA, AgroParisTech, Université Paris-Saclay, 78850, Thiverval-Grignon, France
2 UMR SADAPT, AgroParisTech, INRA, Université Paris-Saclay, 16 rue Claude Bernard, 75231 Paris, France
3 Luxembourg Institute of Science and Technology (LIST), Environmental Research and Innovation (ERIN), 41, rue du Brill, L-4422 Belvaux, Luxembourg

* Corresponding author: Benjamin.Loubet@inra.fr

Abstract. This study reports NO, NO_2 and O_3 mixing ratios and flux measurements using the eddy-covariance method during a 7 month period over an oilseed rape field, spanning an organic and a mineral fertilisation event. Cumulated NO emissions during the whole period were in agreement with previous studies and showed quite low emissions of 0.26 kg N ha^{-1} with an emission factor of 0.27%, estimated as the ratio between total N emitted in form of NO and total N input. The NO emissions were higher following organic fertilisation in August due to conditions favouring nitrification (soil water content around 20% and high temperatures), while mineral fertilisation in February did not result in high emissions. The ozone (O_3) deposition velocity increased significantly after organic fertilisation. The analysis of the chemical and turbulent transport times showed that reactions between NO, NO_2 and O_3 below the measurement height occurred constantly throughout the 7 month period. Following organic fertilisation, the NO ground fluxes were 30% larger than the NO fluxes at the measurement height (3.2 m), while the NO_2 fluxes switched from deposition to uptake during certain periods, being negative at the surface and positive at the measurement height. This phenomenon of "apparent NO_2 emissions" appears to be significant during strong NO emissions and high O_3 ambient mixing ratios, even on a bare soil during August.

Keywords: eddy covariance, chemical reaction, transport time, oilseed rape, NO, O_3, NO_2

1. Introduction

Agricultural soils represent an important source of atmospheric nitric oxide (NO), especially in highly fertilized regions (Oikawa et al., 2015). Global estimates of total NO_x (NO + NO_2) emissions from soils range between 4 and 21 Tg N yr^{-1}, which represents between 10% and 15% of the global NO_x budget (Davidson and Kingerlee, 1997; Houghton et al., 2001; Yienger and Levy, 1995). NO_x inventories are subject to error in magnitude and especially in spatial distributions (Martin et al., 2003), which can be constrained by satellite observations and range around 30% at the global scale (Toenges-Schuller et al., 2006). NO_x emissions are of considerable interest also for atmospheric photochemistry, and acting as ozone (O_3) precursors, they indirectly have an impact on climate. O_3 is indeed an important greenhouse gas, contributing 25% of the anthropogenic net radiative forcing (Forster et al., 2007).

NO_x, and especially NO_2, are toxic gases for humans, exposure to which increases risks of various respiratory diseases. The World Health Organization gives guidelines for NO_2 exposure limits, both annual means (40 $\mu g\ m^{-3}$) and 1-hour mean (200 $\mu g\ m^{-3}$) (Prüss-Üstün et al., 2016). For O_3, only a short-term threshold is given (100 $\mu g\ m^{-3}$ for the 8-hour mean) because there are fewer studies on long-term exposure. These thresholds are established both in epidemiological and toxicological studies on humans and animals. Similarly, nitrogen deposition leads to serious adverse effects on vegetation (eutrophication, biodiversity erosion and acidification being the most serious ones), while O_3 has a direct adverse effect on plant health through oxidation of photosynthesis pathways and direct tissue destruction above large thresholds. For nitrogen, the concept of critical load has been developed which gives the amount of nitrogen deposition above which an ecosystem is impacted. These critical loads range from 5 kg N ha^{-1} yr^{-1} for sensitive habitats to 20 kg N ha^{-1} yr^{-1} for less sensitive ones (APIS, 2016). For these reasons, national and international authorities regulate atmospheric levels of these pollutants.

NO_x emissions from soils are primarily the by-products of nitrification and denitrification processes and the chemical decomposition of HNO_2 (Laville et al., 2005; Meixner, 1997; Remde et al., 1989). Many authors emphasize that for most agricultural soils, nitrification is the dominant process of NO emissions (Bollmann et al., 1999; Dunfield and Knowles, 1999; Godde and Conrad, 2000). Organic and mineral fertilizers, rich in ammonium, increase NO emissions both by stimulating NO production by nitrification and by decreasing NO consumption.

There is a significant knowledge gap in understanding NO_x exchange between agricultural ecosystems and the atmosphere, partly due to a lack of direct measurements over long periods. NO emissions by soils can either be measured by dynamic chambers (Breuninger et al., 2012; Laville et al., 2009; Laville et al., 2011; Pape et al., 2009), aerodynamic gradient (Kramm et al., 1991), or eddy covariance methods (Rummel et al., 2002; Stella et al., 2013a). Each method has its drawbacks and challenges: the dynamic chamber method may change the surface exchange parameters (Pape et al., 2009), and modify the fluxes due to fast reactions between the triad O_3-NO-NO_2, but thoroughly designed Teflon chambers can overcome this problem (Skiba et al., 2009). The aerodynamic gradient method (AGM) is a well-established method applicable to water-soluble compounds such as NH_3 (Milford et al., 2009), but has several biases of which flux divergence due to chemical reaction is the most limiting for NO-NO_2-O_3 (Duyzer et al., 1995; Kramm et al., 1991; Loubet et al., 2013). Non-stationarity and integration time are also limiting (Lenschow et al., 1994; Stella et al., 2012). The eddy covariance method is adapted for measuring NO fluxes. It is however also vulnerable to flux divergence issues due to NO-NO_2-O_3 chemical reactions. It is therefore essential to measure the fluxes and mixing ratios of the three compounds together.

The eddy covariance (EC) method is the state of the art flux measurement method for energy and CO_2 fluxes (Baldocchi, 2003), and due to the development of new analysers such as fast chemiluminescence, quantum cascade lasers absorption spectroscopy, or proton time of flight mass spectrometers (Ammann et al., 2012; Brodeur et al., 2009; Ferrara et al., 2012; Li et al., 2013; Muller et al., 2010b; Park et al., 2014; Peltola et al., 2014; Sintermann et al., 2011; Stella et al., 2013a; Wolfe et al., 2009) it can currently be applied to several other trace gases. The main advantage of the EC method is that it is a "direct" measurement of the flux at a given height, which depends on fewer assumptions than the AGM, namely the Reynolds averaging and ergodicity hypothesis requiring that "*the averaging time must be much larger than the time scales of variation of the air*

velocity" (Corrsin, 1975, see also Kaimal and Finnigan, 1994). This method has been successfully applied for measuring NO fluxes in a limited number of studies (Eugster and Hesterberg, 1996; Lee et al., 2015; Marr et al., 2013; Min et al., 2014; Rummel et al., 2002; Stella et al., 2013a). The main difficulties of EC measurements are the losses that appear at high frequencies due to adsorption of the gas to the tubing system, which depends also on the size of the absorption cell (Eugster and Senn, 1995) and differential advection caused by the radial variation of the mean velocity and simultaneous radial diffusion of the sample gas (Lenschow and Raupach, 1991). Moreover, since NO_2-to-NO photolytic converters typically applied in combination with chemiluminescence analysers have a conversion efficiency below 100%, measuring both NO and NO_2 with such a converter remains a challenge that requires the use of two analysers simultaneously (Lee et al., 2015).

Due to these limitations, simultaneous measurements of NO, NO_2 and O_3 fluxes by eddy covariance have hence seldom been made. To our knowledge, only a few studies report such measurements and none over an arable crop. There is therefore a gap in knowledge as to whether the reactions between NO, NO_2 and O_3 significantly influence the fluxes above crops and how nitrogen application modifies these fluxes and their interactions. Eugster and Senn (1995) report NO_2 fluxes by eddy covariance and analyse the errors of the method. Most studies conducted over forest show moderate to large in-canopy reactions : Andreae et al. (2002) report comprehensive flux measurements in the Amazonian forest showing evidence of within-forest cycling of the nitrogen oxides emitted from the soil. Horii et al. (2004) report NO_x and O_3 fluxes over a temperate deciduous forest showing consistent NO_x deposition. Geddes and Murphy (2014) report such measurements over two mixed hardwood forests in North America, under a very low NO concentrations regime, which shows mainly NO_x deposition with evidence of chemical reactions in the canopy. Min et al. (2014) report such flux measurements over ponderosa pine which shows evidence of within-canopy chemical removal of NO_x. Ammann et al. (2012) report total reactive nitrogen fluxes by eddy covariance above grassland which compared well with dynamic chamber NO and NO_2 fluxes during periods with no NH_3 emissions. Lee et al. (2015) and Marr et al. (2013) report fluxes of NO and NO_2 over urban areas which differ in their comparison with national emissions inventories: while Lee et al. (2015) found fluxes 80% higher than national inventories, the second study found similar fluxes but with large disparities at the local scale.

In this study we are addressing the following questions: (1) is the eddy covariance method suitable for quantifying the seasonal dynamics and diurnal cycles of the NO, NO_2 and O_3 fluxes above a crop rotation? (2) How are organic and mineral fertilisations affecting these fluxes and their dynamics? (3) To what extent are the chemical reactions between NO, NO_2 and O_3 modifying the fluxes above the ground? And finally, (4) why is O_3 deposition increasing following organic fertilisation? Is that a consequence of interactions with NO emissions?

To answer these questions we report measurements of NO, NO_2 and O_3 fluxes by eddy covariance using a system similar to Lee *et al.* (2015) for one month following slurry spreading over a bare soil at the FR-GRI fluxnet and ICOS site (Loubet et al., 2011). The NO and O_3 fluxes were measured over an additional 6 month period to study the seasonality of these fluxes and to measure the fluxes following application of mineral fertiliser.

2. Materials and methods

2.1 Site description and management

The experiment took place in a 19 ha field located at Grignon (48°51' N, 1°58' E), 40 km west of Paris (France) and lasted more than 7 months from 07/08/2012 to 13/03/2013. The field was surrounded by heavy traffic roads on the east, south and south-west. The field belongs to a large farm (buildings at around 450 m to the south west) with around 210 dairy cows, 500 sheep, and a production of approximately 900 lambs. The terrain has a gentle slope of ~1% and the mean annual temperature and precipitation were 10.9°C and 575 mm between 2005 and 2013. The main wind directions are north-west during clear days and southwest during cloudy and rainy days. The soil type is a *luvisol* or loamy clay (25% clay, 70% silt, 5% sand in the top 15 cm). The soil organic carbon content was ~20 g C kg^{-1}, pH (in water) = 7.6, and bulk soil density was 1.3 g m^{-3}, in agreement with previous measurements on the same site (Laville et al., 2009 and 2011, Loubet et al., 2011). High pH values are common in soils over calcareous layers and with high fine fraction content (clay and silt) as is the one of the Grignon site. Indeed, alkalinity fosters the nitrification process and this range of pH is optimum for it to occur (e.g. Nieder and Benbi, 2008). A detailed description of the site can be found in Laville et al. (2009; 2011), and Loubet et al. (2011).

The field was cultivated with winter wheat (a mix of Atlass and Premio species), which was harvested on 3/08/2012 (16.7 Mg ha^{-1} of dry matter). Cattle slurry was applied on the field with a trailing hose from the 18 to the 19/08/2012, at a rate of 42 kg N ha^{-1} of which 78% was ammonium (NH_4^+). The slurry had a very low dry matter content of 3.2% and a C/N ratio of 15.7. The total C applied was 666 kg C ha^{-1}. A gentle tillage was performed on the 29/08/2012 to incorporate the crop and slurry residues and prepare the soil for oilseed rape sowing (variety Adriana) at a density of 35 plants per square meter. The crop developed slowly during the winter with a dry matter above ground (leaf area index) of 37 g m^{-2} (0.65 m^2 m^{-2}) on the 25/10/2012 and 104 g m^{-2} (0.7 m^2 m^{-2}) on the 18/02/2013. The canopy height stayed below 10 cm during the whole winter. Ammonium nitrate pellets were applied on the oilseed rape field on the 20/02/2013 at a rate of 54 kg N ha^{-1}. Two selective herbicides were applied on the 2 (Springbok: 200 g L^{-1} of Metazachlore and 200 g L^{-1} of DMTA-P at 3 L ha^{-1}) and 31/10/2012 (Devin / Cycloxydime: 100 g L^{-1} at 1 L ha^{-1}) which only destroyed the weeds. In December 2012 slug repellent pellets were applied.

2.2 Micrometeorological and ancillary measurements

Meteorological measurements included wind speed, air and soil temperatures and humidity as well as rainfall, global, net and photosynthetic active radiation. The meteorological measurements were performed on a mast (3.17 m high) near the centre of the field and close to the flux measurement site (Fig. 1). Soil was sampled approximately once a month for water content, total nitrogen and mineral nitrogen analysis. Measurements are described in (Loubet et al., 2011) and will not be detailed here.

A simplified sketch of the EC measurement system is shown in Fig. 1. Three-dimensional wind and temperature fluctuations were measured near the centre of the field at 3.17 m above ground by a sonic anemometer (Gill R3 3-axis anemometer, Gill Instruments Limited, UK). A fast response open-path CO_2/H_2O infrared gas analyser (IRGA LI-7500A, LI-COR, USA) installed at a lateral distance of around 0.2 m to the sonic path measured CO_2 and H_2O fluctuations. O_3 mixing ratios were measured by a high-frequency, dry chemiluminescence O_3 detector (NOAA, USA) and its Teflon PFA inlet tube (length = 2.8 m, internal

diameter = 0.32 mm) was positioned in-between the sonic path and the IRGA at a lower height. The high-frequency signals were recorded at 20 Hz by a Labview program developed in the laboratory. In accordance with (Lee et al., 2015), high-frequency (10 Hz) time series of NO and NO_2 were determined by two fast-response and closed-path chemiluminescence NO analysers (CLD 780TR, EcoPhysics, Switzerland), one being coupled to a photolytic converter (blue light converter, BLC, Droplet Measurement Technologies Inc, USA) for the detection of NO_2 (see Fig. 1). The horizontal separation of the trace gas inlets from the sonic path was 20 cm. Air was sampled through two heated and shaded PFA tubes with a length of 20 m and an inner diameter of 9.55 mm. The first CLD was used for measuring NO and the second one connected to the BLC was used for detecting NO_2. Conversion efficiencies for NO_2 to NO of around 30% were achieved. The high-frequency signals of NO, NO_2 and O_3 were calibrated with mixing ratios measured at 30 min time resolution by slow-response analysers (ThermoScientific, Waltham, USA) (Fig. 1). These instruments were calibrated every 3 to 6 weeks using the gas-phase titration (GPT) method and a 17 ppm NO standard (Air Liquide, FR). The fetch of the field site extended at least to 150 m in all directions and a footprint analysis showed that 90% of the time the entire field was in the footprint during neutral and moderately stable or unstable conditions (Loubet et al., 2011). NO and O_3 fast sensors were functioning during the whole campaign (07/08/2012 to 13/03/2013) together with NO, NO_2 and O_3 slow-response analysers and the meteorological station. High frequency NO_2 measurement was performed from 14/08/2012 to 30/09/2012. In this study we focus on two periods: (1) from 14/08/12 to 29/08/12 during which all fluxes were measured and NO fluxes were the highest, in order to investigate the interactions between the fluxes and mixing ratios of the NO-NO_2-O_3 triad, and (2) over the whole period for NO fluxes analysis. **[INSERT FIGURE 1]**

2.3 Eddy covariance fluxes computations

The turbulent fluxes were computed as the covariance between the fluctuations of the scalar of interest and the vertical component of the wind. As the EC method and its theoretical background are described in the literature - e.g. (Foken, 2008) - details will not be provided here.

For closed-path sensors (NO, NO_2 and O_3), the lag time between *w'* and the dry mole fraction χ, had to be determined. This was done by searching for the maximum of the covariance function $(\overline{w'(t)\chi'(t-lag)}$.

The lag for NO was 3.1 s [2.4-3.65 s] (Q50 [Q25-Q75]), for NO_2 it was 4.0 s [3.65-4.55 s], and for O_3 it was 2.9 s [2.5-3.25 s]. The lag was filtered for outliers (points outside of median lag ± standard deviation were considered as outliers) and the covariance was computed as the value of the covariance function at the filtered lag.

As fast-response sensors for NO, NO_2 and O_3 were not absolute, the fluxes were computed following the ratio method for O_3 described by (Muller et al., 2010a), and in accordance with (Lee et al., 2015) for NO and NO_2:

$$F_{O3} = \frac{\overline{\chi_{O3}}}{V_{dry}} \frac{\overline{w'O_3'}}{\overline{O_3}} \quad (1)$$

$$F_{NO} = \frac{\overline{w'NO'}}{S_{NO} V_{dry}} \quad (2)$$

$$F_{NO} = \frac{1}{\alpha V_{dry}} \left(\frac{\overline{w' NO_{x}'}}{S_{NO2}} - \frac{\overline{w' NO'}}{S_{NO}} \right) \quad (3)$$

where O_3(in mV), NO and NO_x (in counts s^{-1}) are the uncalibrated fast signals, χ_{O3} is the 30 min average of the slow-sensor reference O_3 mixing ratio (in ppb), while S_{NO} and S_{NO2} are the sensitivity of the analysers (in counts s^{-1} ppb^{-1}). α is the blue light converter conversion efficiency, and V_{dry} is the molar volume of dry air (in m^3 mol^{-1}). All fluxes (momentum, heat, CO_2, H_2O, NO, NO_2, O_3) were computed by the EddyPro software-version 5 (www.licor.com/eddypro) and final flux data were averaged for 30 min intervals. Evaluation methodologies from the CarboEurope project were applied - see (Aubinet et al., 2000 ; Loubet et al., 2011).

2.4 Spectral corrections and flux uncertainties

Spectral attenuation of the flux is due to differential transport time of the compound in the tube and interaction with tube walls and filter surfaces (Massman and Ibrom, 2008). We tend to minimize this effect by ensuring a large flow rate in the tubes with a Reynolds number well above the critical threshold for turbulence - see (Lenschow and Raupach, 1991) - as well as heating the tubes to around 5°C above ambient temperature. The residence time of the air samples inside the tubing was around 1 s, ensuring low chemical conversions and the Reynolds number was 11700, hence largely in the turbulent range (Re>4000). However, water vapour interaction is still expected, and sensor separation also generates high frequency losses.

The NO, NO_2 and O_3 random instrument noises were estimated as the 1-σ random uncertainty of the signals as in Lenschow (2000), Langford et al. (2015) and Mauder et al. (2008). This is assumed to be "white noise" and hence uncorrelated to itself apart at lag = 0. It is therefore estimated as the difference between the autocorrelation at lag = 0 s and at lag = ± 0.05 s. The flux random uncertainty was itself evaluated as the covariance detection limit. It was determined as the root mean square error of the covariance function over 60 second periods at lag times well away from the position of the time lag. In practice, these were taken at lags larger than 120 s as absolute values as proposed by Langford et al. (2015).

2.5 Chemical reactions, time scales and flux divergence

Chemical reactions between NO, NO_2 and O_3 are important to consider when interpreting the measured fluxes as they can affect the fluxes above the ground. A common way to determine whether these reactions may indeed affect the flux is through comparison of chemical and transport time scales. Details of the reactions rates, time scales and flux divergence calculations are given in the supplementary material sections S1-S3.

3. Results and discussion

3.1 Quality check and uncertainties in NO, NO_2 and O_3 flux measurements

NOx and O_3 half-hourly fluxes were filtered by the quality check test included in EddyPro (www.licor.com/eddypro), according to the 0-1-2 labelling proposed by Mauder and Foken (2006), that includes tests for stationarity and for well-developed turbulence. As recommended in the framework of the CarboEurope project, we discarded fluxes with a quality check index value of 2. This led to keeping 74%, 84% and 76% of the records for NO, O_3 and NO_2 respectively. The total records of NO and O_3 half-hourly fluxes were 11329 (from 07/08/2012 to 13/03/2013), while for NO_2 they were 2257 (during the period 14/08/2012 to 30/09/2012).

The largest systematic uncertainties were the high frequency losses, which were estimated with the in-situ ogive method (Ammann et al., 2006), and amounted to 10% for O_3, 20% for NO and 30% for NO_2 on average over the August-September period (when all fluxes were measured, see Fig. 2). As a bias, they can be corrected for, and this was performed in the following sections of this manuscript. **[INSERT FIGURE 2]**

The second largest uncertainties were the random uncertainties which were lower than 20% in most cases for O_3, NO (and similar to H_2O) and around 30% to 40% for NO_2 (Fig. 3). For NO and NO_2 the random uncertainties peaked during the morning traffic hour around 6:00-8:00 UTC, which is explained by the non-stationarity generated by the local traffic on the mixing ratios. Hence overall the eddy covariance method proved to be usable for measuring NO fluxes over part of the season with an overall uncertainty similar to H_2O. A higher random uncertainty was found for NO_2 fluxes which were smaller than NO fluxes and with a relatively low conversion ratio from NO_2 to NO (30%). **[INSERT FIGURE 3]**

3.2 Meteorological conditions

Daily averages of the air temperature decreased during the measurement period, starting from about 20°C in summer and reaching minima around -5°C from December to March. Daily averages of global radiation decreased from 250 W m^{-2} in August to around 0 W m^{-2} in December, back to around 150 W m^{-2} in the end of March (Fig. 4). The daily average of the relative humidity was around 65% in August and September, and it increased to about 85% for the rest of the period. The wettest period was between October and November, and cumulative rain was 319 mm over the 7 month period, which is quite high. The prevailing wind direction was south-west while the most intense winds were observed from north and south (Fig. S2). Figure S2 also shows that wind regimes were quite different in summer and winter: prevailing wind directions during August and February were from south-west and north-east, respectively. Soil water content (SWC) ranged between 20% and 40% (volume) (Fig. 4), with a long period between October and January with values around 28%, and increased further in January to 35%, with sharp decrease during some periods. **[INSERT FIGURE 4]**

3.3 Seasonal dynamics and diurnal cycles of the NO, NO_2 and O_3 fluxes above a crop rotation

3.3.1 Seasonal dynamics of NO-NO_2-O_3 mixing ratios

Average daily NO, NO_2 and O_3 mixing ratios were 3.6, 6.9 and 24.8 ppb, respectively. The NO and NO_2 mixing ratios were higher when winds blew from the east (from the direction of Paris), while O_3 showed the opposite behaviour, which can be explained by depletion of O_3 by NO sources from the surrounding traffic (as shown in Fig. S2) and by reactions (S1-S2). Daily NO_2 / NO_x ratios were on average 66%, which is typical for traffic and urban pollution (Carslaw, 2005; Minoura and Ito, 2010), and ranged from 4% to 93% during the entire period. The NO_2 mixing ratio was significantly higher (Student t-test p-value lower than 8 10^{-11}) than the NO mixing ratios in August and early September, end of January and mid-February, and end of March. During sporadic episodes, NO peaks were of the same order or even higher than NO_2 peaks (Fig. 4).

3.3.2 Seasonal dynamics of NO NO_2 and O_3 fluxes

The daily averaged NO fluxes were very small, except during a period of strong emission following organic fertilisation over two days in August (18-19/08/2012), with maximum daily average fluxes of around 1.5 nmol m^{-2} s^{-1} (Fig. 4). Other emissions episodes, including mineral fertilisation in February (20/02/2013),

were characterized by mean daily fluxes below 0.5 nmol m^{-2} s^{-1}. The NO fluxes were slightly negative for some events (Q25, Q50 and Q75 equal -0.013, 0.031 and 0.11 nmol m^{-2} s^{-1}, Fig. S3). The O_3 fluxes ranged between -13.8 and 0 nmol m^{-2} s^{-1}, and averaged to -3.12 nmol m^{-2} s^{-1}. The largest O_3 deposition fluxes were observed following organic fertilisation in August, and were correlated with the highest NO emissions. This period also corresponded to large daily O_3 mixing ratios (Fig. 4). The NO_2 fluxes were only measured during the first one and a half months (16/08/2012 to 30/09/2012) and were mostly negative (indicating deposition), except during the first week following organic fertilisation (Q25, Q50 and Q75 equal -0.11, -0.07 and 0.08 nmol m^{-2} s^{-1}) (Fig. S3). O_3 fluxes were in the same range of magnitude, typically between -20 and 0 nmol m^{-2} s^{-1}, as those reported by previous studies at the same site (Stella et al., 2013b; Stella et al., 2011b; Tuzet et al., 2011) and in the literature over various canopies such as grassland (Stella et al., 2013a), barley (Gerosa et al., 2004), potato field (Coyle et al., 2009), or forests (Fares et al., 2010; Gerosa et al., 2005), although O_3 flux magnitude is sharply dependent on local O_3 mixing ratio. We found similar magnitudes of ozone fluxes in August and September as those reported by Stella et al. (2013) over a meadow during the summer. We also found similar nocturnal O_3 deposition velocity as found by Stella et al. (2011) over bare soil during summer, but with a higher daily maximum (0.8 cm s-1 instead of 0.5-0.6 cm s-1). Seasonal and daily dynamics of O_3 deposition velocity are shown in Fig. 5. We further find a similar midday magnitude as Stella et al. (2011) found in April with wetter soils. Night-time ozone deposition velocity did not go lower than around 0.2 cm s^{-1} in our study, as also found by Zhu et al. (2015) over a growing wheat in China, Stella et al. (2011) over bare soil in summer, and Lamaud et al. (2009) over maize. These authors as well as Huang et al. (2016) clearly show that this is due to non-stomatal deposition being primarily driven by u_* which does not reach zero at night during these periods. We can hence conclude that we found consistent ozone deposition in August and September compared to other studies at that site or in other geographical areas. When compared to previous years at the same site the deposition velocity measured during the winter in this study was clearly smaller. We interpret this as being primarily due to u_* being smaller that winter compared to other winters, as well as due to a bad development of the winter crop due to soil drought in September (SWC =20% in the 15 cm horizon).

[INSERT FIGURE 5]

3.3.3 Comparison of ozone fluxes to the Stella et al. (2011) parameterisation over soil

In order to compare to previous studies of ozone deposition onto bare soil on the same site, we have calculated the soil surface resistance as in Stella et al. (2011) and deduced the ozone deposition velocity as $V_{dO3} = (R_{soilO3} + R_{bO3} + R_a(z_{ref}))^{-1}$. In this way, we can compare the two studies while excluding any confounding factors (roughness and turbulent exchange intensity). We can see in Fig. 6a that the measured ozone deposition velocity during August follows the parameterisation of Stella et al. (2011) most of the time except for some days including 18 and 19 August which corresponds to slurry application and 24, 25, 26 August, which follows a small rainfall. We also see an overestimation of the Stella parameterisation before the 18 August, which we interpret as being due to the straw and wheat residues being present on the ground before slurry incorporation. This comparison hence demonstrates that the ozone deposition was indeed increased slightly following slurry application and subsequently following rainfall. This may be either due to a physical reason (increased surface exchange on the soil due to tillage or humidity change due to slurry) or a chemical reason (surface reactivity changes due to added organic matter or VOC emissions from the slurry). Fig. 6b further shows that the main

differences are observed for wet soils and relatively low temperatures (this is after rainfall) and to a lesser extent for dryer and hotter situation (following slurry spreading).

[INSERT FIGURE 6a and 6b]

3.3.4 Diurnal cycles of mixing ratios and fluxes over periods of interest

O_3 mixing ratios exhibited a typical diurnal cycle that was governed by photochemistry and convective mixing within the boundary layer and from the free troposphere during daytime. It started to increase with sunlight around 7 a.m., and declined in the evening starting from 6 p.m. due to lack of photochemical formation in the absence of sunlight, as well as deposition and destruction with NO in this high NO_x emission area. In general, NO mixing ratios featured a marked peak in the early morning and remained high until around 13:00 UTC (Fig. 7b). During the early afternoon, the O_3 increase was correlated with the NO decrease. NO_2 mixing ratios showed a bi-modal diurnal cycle with its maxima in correspondence with morning and evening traffic peaks, i.e. around 6 a.m. and 7 p.m..

The NO fluxes also showed a diurnal cycle similar to the one of soil temperature with an emission peak around 12 a.m. (Fig. 7a and b). This suggests that NO emissions are related to nitrification, for which the emission rate is an exponential function of soil temperature (Henault et al., 2005). This was already shown for the Grignon soil by Laville et al. (2011). The fact that NO fluxes decrease earlier than soil temperature is most likely due to titration of NO by O_3 in the late morning and early afternoon, causing the NO emissions at the reference height to be reduced with respect to ground emissions. After correction for chemical reactions the NO emissions diurnal cycle is indeed at a peak later in the day, more in phase with ground temperature (see Fig. 11). This is also indicated by the positive NO_2 flux observed during the same time of the day. The O_3 flux was mainly negative (deposition) and follows the diurnal dynamics of measured mixing ratios. **In terms of deposition velocity, the ozone deposition velocity followed a clear diurnal cycle with a maximum during the day and a minimum at night. The measured NO_2 deposition velocity showed slightly negative values, but slightly positive ones when corrected for reactions with NO and O_3.**

[INSERT FIGURE 7a and 7b]

3.4 Influence of organic and mineral fertilisations on NO emissions

The NO flux averaged over the whole period was 0.09 nmol m^{-2} s^{-1} (mean), which is in the range of previous findings for the same site. Laville (2011) and Loubet et al. (2011) reported yearly averaged NO fluxes varying between 0.07 and 0.15 nmol m^{-2} s^{-1} for 2007-2009. The NO flux distribution was shifted towards positive values after the organic fertilisation in August (Fig. S3), with the mean NO flux during the two weeks following the fertilisation (0.49 nmol m^{-2} s^{-1}) being six times larger than the one for the whole period. For the same period, the ozone flux distribution was shifted towards more negative values. Figure S3 also shows that flux distributions after mineral fertilization do not differ much from the ones relative to the whole period. During the two weeks following the February mineral fertilisation the NO flux increased less and was only 1.7 larger than over the whole period (0.14 nmol m^{-2} s^{-1}). These numbers are also in line with those reported following fertilisation on the same soil in the 2007-2009 period by Laville (2011) and Loubet et al. (2011), which also showed some periods with slightly negative NO fluxes. Stella et al. (2012) measured a larger peak of NO

emissions following slurry spreading, but only lasting two to three days, which was probably due to a dryer soil in our study compared to Stella et al. (2012).

Following the slurry application, the NO emissions amounted to 0.1 kg N ha^{-1}, which represents 0.24% of the applied nitrogen (42 kg N). Following the mineral fertilisation, the NO emissions amounted to 0.02 kg N ha^{-1}, which represents 0.037% of the applied nitrogen (54 kg N). Over the whole period from August 2012 to March 2013, we evaluate a loss of 0.26 kg N ha^{-1}. With a total N input of 96 kg N ha^{-1}, this gives an estimate of the NO emission factor of 0.27%, which is similar to values reported earlier for the same site (Laville et al., 2011) but one order of magnitude larger than the EMEP/IPCC default value of 0.04. Nevertheless, this is an average value calculated with the Tier 1 approach, which does not take into account correction factors depending on soil pH or fertilizer type. This more detailed approach, the Tier 2, has not been developed for NO (EEA, 2016).

The reasons for lower emissions following winter mineral fertilisation than following summer manure application are manifold. Even if the amount of applied nitrogen was similar for the two cases (42 and 54 kg N ha^{-1}), meteorological and soil conditions were much more favourable for nitrification in summer than in winter (Davidson, 1992; Williams and Fehsenfeld, 1991). Indeed, NO emissions from agricultural soils are primarily the by-products of nitrification, and this hypothesis was tested for the Grignon site by Laville et al., (2011). Nitrification is inhibited by low soil temperature and high water content that causes anoxia. Soil temperature was much lower in February than in August (2.5 compared to 20 °C on average). February was particularly humid, with a total precipitation of 10 mm, while in August no significant rain event occurred after the first week. In this period indeed, the soil was only humidified by the organic manure supply (on a 4.8 mm thick layer) that was applied on a dry soil. The soil water content at 5 cm depth in September 2012 was around 21% in volume, while in February it was 33% in volume. These two factors led to more favourable conditions for nitrification in August than in February.

3.5 Influence of surrounding roads on the measured fluxes and concentrations of the NO-NO_2-O_3 triad

Using the FIDES flux and concentration footprint model (Loubet et al., 2010) we evaluated the footprint of nearby roads. Overall the flux footprint from the nearby roads was smaller than 1% (which means that only 1% of the road emissions contributes to the flux at the mast) most of the time, but the concentration footprint reaches up to 10% during some episodes, with separate roads contributing differently depending on the period (Fig. S1). Assuming a conservative emission of 250 mg km^{-1} $vehicle^{-1}$ and an average vehicle count of 10000 vehicles per day (2010 counts, “Statistiques du département des Yvelines pour 2010” ranges between 5000 and 15000), we evaluate that the roads contribute from 4% to 40% to the measured fluxes. However, since vehicles emissions of NO_x have a sporadic nature, 10000 vehicles per day means a maximum of ~1 vehicle every 2 seconds (if we consider, conservatively, that most of the traffic is condensed during 9 hours only). These vehicles are also moving at about 90 km h^{-1} (25 m s^{-1}), hence leading to a moving point source of NO_x. We therefore expect that the signal of this moving and sporadic source is not captured by the eddy-covariance method, and would be filtered out by despiking and flux calculation procedures (Foken, 2008 ; Mahrt, 2010).

3.6 Chemical interactions: the NO-NO_2-O_3 triad and effect on the fluxes

In order to investigate the interactions between the fluxes and mixing ratios of the NO-NO_2-O_3 triad, we focus on the period from 14/08/12 to 29/08/12, during which all fluxes were measured and NO fluxes were the highest.

The two weeks following the organic manure application (from 18/08 to 19/08) are characterized by hot sunny days, with maximal global radiation above 800 W m^{-2}, except for 24/08 when the only rain event occurred (Fig. 8). The period of August 18th to the 23rd was the warmest, with soil surface temperatures above 40°C at noon during most days, while the air temperature decreased from around 35°C to around 20°C during the same period. The soil temperature at 5 cm depth followed the same trend, but with a lower daily maximum and a higher night-time minimum. Due to sensor breakdown the soil water content was not measured during this period. The small latent heat flux (LE) after the 19th of August, (17 W m^{-2} on average between August 19th and the 31st) the large sensible heat flux (60 W m^{-2} on average) and radiation (212 W m^{-2} on average) indicate that the soil humidity of the top soil layer was low. Hence, we assume that the SWC was probably similar to what was measured in September (around 20 % in volume), which is ideal for nitrification to occur (Laville et al., 2011; Oswald et al., 2013). **[INSERT FIGURE 8]**

The 18/08 was the first day when NO emissions from the soil occurred. The emissions lasted around two weeks following the organic fertilisation (Fig. 4), during which the NO flux during daytime exceeded 0.5 nmol m^{-2} s^{-1}, peaking around 12 a.m. The nocturnal NO flux usually decreased to zero, except for the night of 25/08, characterized by strong winds (Fig. 8). The maximum of the NO emissions was 2.7 nmol m^{-2} s^{-1} observed six days after fertilisation on 21/08.

The NO_2 flux daily pattern was different during the two weeks following organic manure application compared to the period before (Fig. 8). It was in general positive during the day and around zero at night during the period from 18/08 to 29/08, except for the night of 25/08 when it was large and negative. Positive NO_2 fluxes might be explained by chemical reactions between NO and O_3 in the surface layer (De Arellano et al., 1993), which will be discussed in the next section.

The O_3 flux was also significantly higher (Student t-test p-value lower than $2\ 10^{-16}$) following organic fertilisation (mean -10.7 nmol m^{-2} s^{-1}) than during the rest of the experimental campaign (mean -3.1 nmol m^{-2} s^{-1}) (Fig. S3). Since the mixing ratio of O_3 was quite variable during the campaign (Fig. 4), it is more interesting to look at the deposition velocity which underpins the surface exchange processes (Fig. 7b and 8). The median V_{dO3} during the organic fertilisation event exceeded the median over the rest of the experimental campaign by a factor of two. However, this increase in O_3 deposition velocity cannot be explained by reaction with soil-emitted NO alone as the O_3 flux is an order of magnitude larger than the NO flux.

Different pathways for the near-surface O_3 removal are likely: i) photolysis of O_3 by ultraviolet light in the presence of water vapor forming OH radicals, ii) gas phase reactions with reactive VOCs and iii) heterogeneous reactions with the soil or with molecules adsorbed on soil..

The NO mixing ratio was well correlated with the NO flux, with a normal correlation coefficient of 40% for the two weeks following the organic fertilisation (excluding 24-25 August), while it was only 2% for the 7 month period. This suggests that, following fertilisation, the ambient NO levels were mainly due to local emissions. The NO_2 mixing ratio was less correlated with the NO_2 flux, suggesting that NO_2 levels were more related to advection from surrounding road traffic than from local emissions. Indeed, both NO and NO_2 are

emitted from road traffic and urban pollution, but the NO_2 component quickly becomes prevalent as the plume is advected, especially in presence of high O_3 levels, as in our case (Carslaw, 2005; Minoura and Ito, 2010). The minimum night-time mixing ratio is mainly controlled by night-time wind velocity: the higher the night-time velocity, the higher the mixing ratio, due to a better mixing in the atmospheric surface layer. During conditions with lower wind speed, deposition and reaction with local NO_x sources lead to a high depletion of O_3 during the night.

3.7 To what extent are the chemical reactions between NO, NO_2 and O_3 modifying the fluxes above the ground?

Measured mixing ratios and fluxes of NO, NO_2 and O_3 are affected by chemical reactions (S1 to S4) in addition to emissions and deposition processes. Especially, the diurnal fluxes of NO_2 observed from the 18 to the 23 of August, were positive (emissions) and of the same order of magnitude as the NO fluxes, while they were negative afterwards. The simultaneous observation of positive NO and NO_2 fluxes are typical for the NO-to-NO_2 transformation below the flux observation level in the presence of high O_3 mixing ratios. This phenomenon is called "apparent NO_2 emissions" and was observed in other studies mainly above dense or tall canopies (Ammann et al., 2012; Min et al., 2014; Plake et al., 2015). For the reactions (S1-S2) to occur below the measurement height, the turbulent transport time (τ_{trans}) needs to exceed the chemical reaction time (τ_{chem}) (Arellano and Duynkerke, 1992; De Arellano et al., 1993; Lenschow and Delany, 1987; Plake et al., 2015; Stella et al., 2013a; Stella et al., 2011a; Stella et al., 2012). The Damköhler number $Da = \tau_{trans} / \tau_{chem}$ is often used to determine the conditions favourable for chemical reactions: in cases when Da is higher than unity chemical reactions are faster than the transport (flux divergence), whereas Da values smaller than 0.1 indicate that the influence of chemical reactions was negligible. The aerodynamic resistance $R_a(z)$ (Eq. S8) was overall quite small and ranging from 45 to 128 s m^{-1} (1st and 3rd quantiles), hence leading to a quite short transport time scale (but larger than 100 s most of the time). The boundary layer resistance was around 22 and 43 s m^{-1} (1st and 3rd quantiles) for O_3 (Fig. 9). The surface resistance for O_3 was estimated as $R_{soil}(O_3) = V_{dO3}^{-1} - R_a - R_b(O_3)$, and dominated the other resistances (100 to 480 s m^{-1}). The O_3 penetration depth in the soil was estimated as the depth necessary to explain the measured $R_{soil}(O_3)$ if molecular diffusion in the soil pores is the main limitation factor. In practice this corresponded to the dry soil layer used in (Personne et al., 2009). This depth ranged from 2 to 10 mm on average and was smaller at noon than during the night (Fig. 9). Overall, the chemical time τ_{chem} and the transport time τ_{trans} were of the same order of magnitude at any time of the day between applications and during mineral fertilisation, and τ_{chem} was smaller than τ_{trans} during the organic fertilisation. As a consequence, the Damköhler number was around unity most of the time and larger than unity during the organic fertilisation period, showing that the reaction between O_3, NO and NO_2 happened during transport from the ground to the EC measurement height at all times at this site. During the fertilisation event, the Damköhler number was especially high at night, when the transport time increased more substantially than the chemical timescale. These results are similar to findings by Stella et al. (2012) for the same site over bare soil. During the periods with vegetation, the increase of the transport time scale above the canopy was less than that of the chemical time scale during nighttime, as the presence of vegetation increases the mixing, and, hence diminishes $R_a(z)$. **[INSERT FIGURE 9]**

The Damköhler number shows that NO reacts with O_3 and that photolysis also plays a role. How does this affect the NO flux measured at the reference height compared to the one at the ground? We quantified this variation by numerically solving Eq. S13, based on the model of Duyzer et al. (1995). Due to the reaction with O_3, the calculated NO flux at the ground surface was on average 32% larger than that at the measurement height during the period 17-29/08 (0.93 instead of 0.63 nmol m^{-2} s^{-1}). This would represent an increase of 37 g of N emission following slurry spreading. For NO_2, the calculated flux at the ground surface was mostly negative while it was mainly positive at the reference height during the period 18-22/08. On average the NO_2 flux at the ground was -0.33 nmol m^{-2} s^{-1} over the period 17-29/08 while it was -0.03 nmol m^{-2} s^{-1} at the reference height. For NO fluxes, the major discrepancy between fluxes at the surface and the measurement height occurs during periods with relatively large and stable values of the Damköhler number (Fig. 10), as this is the case when chemical reactions consume NO before it reaches the measurement height.

[INSERT FIGURE 10]

The derivation of surface fluxes with the Duyzer model also leads to a diurnal cycle of the NO flux that is closer to the one observed for ground temperature, corroborating the hypothesis that ground emissions are mostly due to nitrification for our site (Fig. 11).

[INSERT FIGURE 11]

Since the O_3 deposition flux was much larger than the NO flux, the reaction with NO changed the absolute value by only 3% when comparing the flux at the measurement height to the ground surface. Indeed, as only reactions (S1) and (S2) are considered in eqs. (S12) and (S13), which we used to numerically evaluate surface fluxes, we obtain: $\Delta[FNO] = \Delta[FO_3] = -\Delta[FNO_2] = 0.3$ nmol m^{-2} s^{-1} where Δ stands for the difference between surface and measurement height.

3.8 Why is O_3 deposition increasing following organic fertilisation?

We observed that following organic fertilisation (performed by injection and hence soil tillage), O_3 deposition increased by a factor of two (as shown by the deposition velocity, Figs. 9 and 10). Several hypotheses may explain this increase: (1) the increased surface exchange due to soil tillage, (2) the reaction with NO emitted by the ground, and (3) the reaction with VOCs emitted by the ground:

A first hypothesis (1) would be that the increase in deposition velocity following the organic fertilization could be due to a change in physical characteristics of the soil surface. Indeed, the application of cattle slurry with a trailing hose modifies the soil structure at the surface which consequently increases the available surface for O_3 deposition, and therefore the deposition velocity. This hypothesis is consistent with the comparison of measured deposition velocities and modelled deposition velocities using the Stella et al. (2011a) R_{soil} parameterization (see sect. 3.3.3 and Figure 6a). Indeed, while there is a good agreement between measured and modelled V_d after the 26th of August (i.e., after the rainfall event), modelled V_d systematically underestimates measured V_d between slurry application and the rainfall event. Since the parameterization of R_{soil} was obtained for the Grignon site over different periods, that means R_{soil} accounts for the mean soil structure of the Grignon site. Therefore, it can be hypothesized that (i) R_{soil} is underestimated from slurry application to the rainfall event due to the change of

soil surface structure, and (ii) after the rainfall event, the soil surface recovers its mean structure corresponding to the R_{soil} parameterization.

A second hypothesis (2) would be that O_3 would react with NO emitted by the soil. Although the reactions with NO during transport are shown to be small compared to the NO flux (Figure 10), reactions in the soil surface layer may be more significant due to large NO concentrations in the soil, despite the fact that this layer is very small. A graph of the difference between the measured and the modelled ozone flux following fertilisation (Fig. S4) seems to show that the additional O_3 deposition is correlated with the NO flux. This would mean that the NO_2 produced in the soil by reaction with NO would be adsorbed on the soil surface either in the mineral phase or dissolved in the water phase as NO_2. To evaluate this assumption further, we evaluated the Damköhler number in the soil surface layer by assuming that the layer depth is equal to the O_3 penetration depth δ_{O3soil} (Fig. 9). In this layer the transport time is equal to soil resistance for O_3 times the penetration depth $R_{soilO3} \times \delta_{O3soil}$. We can evaluate the NO mixing ratio that would explain the additional O_3 destruction at the surface, by searching for the value of $[NO]_{soil}$that satisfies $\tau_{trans}(Soil, O_3) = \tau_{chem}(Soil, O_3)$. By doing so, we found that $[NO]_{soil}$ would need to reach 5 to 40 ppm to explain the increase in O_3 deposition following organic fertilisation. Gut *et al.* (1998) and Gut *et al.* (1999) measured NO mixing ratios at a 2 cm depth in the soil under wheat with the membrane tube technique and report mixing ratios around 100 ppb and always below 400 ppb following fertilisation, which is one to two orders of magnitude below the mixing ratio which would be needed to explain the observed O_3 flux. Moreover, the rate of NO production in the soil surface layer would have to be equal to the O_3 flux to the ground (around 20 nmol m^{-2} s^{-1}) which is an order of magnitude larger than what Gut *et al.* (1998) or Laville *et al.* (2009) report as maximum NO flux. However we should stress that both Gut *et al.* and Laville *et al.* report NO fluxes that were measured in the presence of ozone and hence would have been depleted by reaction with it in a similar way as here.

A third hypothesis would be that O_3 would react with VOCs emitted by the ground. Reactive VOCs such as sesquiterpenes and monoterpenes were previously found to be emitted from soils (Horvath et al., 2012; Penuelas et al., 2014), and some of these sesquiterpene species react with O_3 in the order of a few seconds. The reactions of O_3 with larger terpenes are important sources of OH, as well as the ozonolysis of simpler unsaturated compounds. (Donahue et al., 2005). Currently, there is little or no data available on the emission of VOCs from slurry application. However, a recent study mainly focusing on quantification of odor emissions from soil application of manure slurry, showed the formation of a certain number of VOCs, included organic sulfur compounds, carboxylic acids, alcohols, carbonyl compounds (ketones and aldehydes), aromatic compounds (phenols and indoles) and nitrogen compounds (Feilberg et al., 2015). Based on their analyses, the compound most responsible for the overall odor impact from the VOC emissions was 4-methylphenol. These authors also showed the emission of trimethylamine, a compound that can react quickly with O_3, leading to formation of secondary organic aerosols (Murphy et al., 2007). Furthermore, these authors suggest that a large part of these VOCs are formed through ozonation reactions (i.e. byproducts of ozonation: methanol, acetone, and acetaldehyde). Indeed, the slurry would be transported downwards through the soil, where efficient heterogeneous reactions can take place at particle interfaces. It has been shown that the heterogeneous reaction probabilities may be much greater than anticipated. For example, measurements on oxide surfaces with a chemical structure commonly found in VOCs (i.e. alkenes, terpenes, carbonyls) showed that the O_3 reaction probability of a surface-attached alkene can be up to five orders of magnitude greater than for the same reaction

in the gas-phase (Stokes et al., 2008). In the same way, Fick et al. (2005) observed that ozonolysis reaction rates of some terpenes were much higher than predicted, possibly as a result of reactions on the surfaces used in their experiments. These results suggest that terpenes can remain on the surfaces, enhancing the O_3 reactivity. Similarly, some other authors observed that surface reaction probabilities with O_3 were 10 to 120 times greater than their corresponding gas-phase values (Dubowski et al., 2004; Springs et al., 2011). It is also known that soils can act as a sink of VOCs, by their adsorption to soil mineral particle surfaces and humic substances (Penuelas et al., 2014). Hence, it is likely that surface chemistry including photo-enhanced O_3 uptake on organic matter (Jammoul et al., 2008; Reeser et al., 2009) may explain the increase in O_3 deposition, a process not yet described in the literature. It may also be likely that O_3 is destroyed by very reactive VOCs in the gas phase as hypothesized by Wolfe et al. (2011). These gas-phase reactions, however, require that the chemical reaction time to be shorter than the turbulence transport time (Plake et al., 2015; Stella et al., 2012).

However, our study does not allow us to conclude definitively which of the three hypotheses is the most likely.

4. Conclusions

Eddy covariance flux measurements of the NO-NO_2-O_3 triad during a 7 months period allowed evaluating several mechanisms controlling the exchange of these reactive trace gases with an agricultural soil. Eddy covariance technique proved to be suitable at capturing seasonal and diurnal dynamics of the fluxes, and allowed to interpret flux behaviour according to meteorological variables, fertilisation practices and chemical reactions. Nevertheless, random uncertainty was particularly important (>20%) during morning traffic peaks due to non-stationarity of NO_x and O_3 mixing ratios. As concerns NO_2, uncertainty was even higher (up to 40%) due to the indirect measurement method. We thus recommend caution in the use of the method in non-stationary conditions, and combined measurements of horizontal gradients of mixing ratios to quantify the effect of advection. Also, additional measurements of surface mixing ratios would be useful to check the reconstruction of surface fluxes that we performed by using the logarithmic-profile model of Duyzer. Finally, high NO_2 to NO conversion efficiency should be assured to reduce uncertainty of NO_2 fluxes.

In particular, the magnitude and temporal variability of NO emission fluxes following two fertilisation episodes were analysed, one in summer and the other one in winter. Mean NO emissions during the whole period were in agreement with previous studies on the same site. Emissions were significantly higher (Student t-test p-value lower than $2\ 10^{-16}$, and a factor of seven difference on the mean) during two weeks following organic fertilisation in August than during the rest of the experimental period. These large emissions are mainly due to favourable conditions for nitrification: soil water content around 20% and high temperatures. In February, following mineral fertilisation, the increase of NO emissions was less pronounced, although the same amount of N was applied. This difference is likely due to less favourable conditions for nitrification in February (low temperature and higher soil water content), rather than to the different form of fertilizer. On average over the whole period, we derived a loss of 0.26 kg N ha^{-1} as NO from the field. With a total N input of 96 kg N ha^{-1}, this results in an NO emission factor of 0.27%, which is in the lower range of earlier reported values on this site (Laville et al., 2011).

Our findings show that NO emissions from agricultural soils are limited (0.27% of the N-NO applied over the 7 month period, which with a conservative estimation can be extended to a yearly amount). When

hypothetically extended to France with an average nitrogen fertiliser use of 80 kg N ha^{-1} over a fertilised area of around 26 Mha, this would lead to a total emission of NO_x of around 5.6 kt N-NO. This is negligible compared to national emissions which are around 240 kt N-NO (CITEPA, 2015). The seasonality and spatial distribution of these emissions may, however, lead to air quality issues during spring and late summer-autumn which are the main fertiliser application periods in rural environments. Indeed, most of the emissions we measured occurred within a few weeks following fertilisation. In terms of ozone, our findings are in accordance with previous ones, showing that ozone is efficiently deposited throughout the year. This means that crops are participating through this process in the reduction of the atmospheric oxidising capacity.

The O_3 deposition velocity was significantly higher following organic fertilisation than during the rest of the experiment (Student t-test p-value lower than 2 10^{-16} and a factor 3 difference on the mean), despite the fact that vegetation was absent. This increase in O_3 deposition could not be explained by the reaction of O_3 with NO in the atmosphere as the NO flux was an order of magnitude smaller than that of O_3. The process behind this ozone deposition increase remains to be discovered. We hypothesised three underlying processes: (1) increase in soil surface due to soil tillage, (2) reaction with NO in the soil layer, and, (3) reactions of O_3 with VOCs emitted by the slurry. None of these hypotheses can be dismissed and further investigation is required. Experiments in controlled conditions are desirable to better understand these processes.

The evaluation of the chemical and turbulent transport times showed that reactions between NO, NO_2 and O_3 below the measurement height occurred during the whole measurement period, leading to a depletion of NO and a build-up of NO_2 from the ground to the measurement height. Following organic manure application, NO fluxes were reduced by 30% from the surface to measurement height, while the NO_2 fluxes switched from deposition to uptake, being negative at the surface and positive at the measurement height. This phenomenon of "apparent NO_2 emissions" was reported in other studies, especially above forests. Here it also appears to be important above a bare soil and at moderate measurement heights, during conditions of strong NO emissions and high ambient O_3 mixing ratios.

Acknowledgements

This work was funded by the FP7 projects ECLAIRE (grant number 282910) and INGOS (grant agreement 284274), the French ANR project ANAEE, as well as ICOS France. The authors acknowledge the director of the AgroParsiTech Farm Dominique Tristan for allowing access to the field. We are grateful to the Max Planck Institute for Chemistry (Mainz, Germany) for the loan of a CLD 780TR analyser for the duration of the experiment. We also thank Gerardo Fratini for the precious support on issues concerning EddyPro, and Christof Ammann and Veronika Wolff for fruitful discussion about NO_x-O_3 chemical reactions. We also thank Polina Voylokov for her thorough correction of the manuscript and Anaïs Durand for helping on NO emission inventory evaluations.

References

Ammann, C., Brunner, A., Spirig, C., and Neftel, A.: Technical note: Water vapour concentration and flux measurements with PTR-MS, Atmos Chem Phys, 6, 4643-4651, 2006.

Ammann, C., Wolff, V., Marx, O., Bruemmer, C., and Neftel, A.: Measuring the biosphere-atmosphere exchange of total reactive nitrogen by eddy covariance, Biogeosciences, 9, 4247-4261, 2012.

606 Andreae, M. O., Artaxo, P., Brandao, C., Carswell, F. E., Ciccioli, P., da Costa, A. L., Culf, A. D., Esteves, J. L.,
607 Gash, J. H. C., Grace, J., Kabat, P., Lelieveld, J., Malhi, Y., Manzi, A. O., Meixner, F. X., Nobre, A. D.,
608 Nobre, C., Ruivo, M. D. L. P., Silva-Dias, M. A., Stefani, P., Valentini, R., von Jouanne, J., and
609 Waterloo, M. J.: Biogeochemical cycling of carbon, water, energy, trace gases, and aerosols in
610 Amazonia: The LBA-EUSTACH experiments, Journal of Geophysical Research-Atmospheres, 107,
611 2002.
612 Arellano, J. and Duynkerke, P. G.: Influence of chemistry on the flux-gradient relationships for the NO-O3-NO2
613 system, Bound-Lay Meteorol, 61, 375-387, 1992.
614 Aubinet, M., Grelle, A., Ibrom, A., Rannik, U., Moncrieff, J., Foken, T., Kowalski, A. S., Martin, P. H.,
615 Berbigier, P., Bernhofer, C., Clement, R., Elbers, J., Granier, A., Grunwald, T., Morgenstern, K.,
616 Pilegaard, K., Rebmann, C., Snijders, W., Valentini, R., and Vesala, T.: Estimates of the annual net
617 carbon and water exchange of forests: The EUROFLUX methodology, Adv Ecol Res, 30, 113-175,
618 2000.
619 Baldocchi, D. D.: Assessing the eddy covariance technique for evaluating carbon dioxide exchange rates of
620 ecosystems: past, present and future, Global Change Biology, 9, 479-492, 2003.
621 Bollmann, A., Koschorreck, M., Meuser, K., and Conrad, R.: Comparison of two different methods to measure
622 nitric oxide turnover in soils, Biology and Fertility of Soils, 29, 104-110, 1999.
623 Breuninger, C., Oswald, R., Kesselmeier, J., and Meixner, F. X.: The dynamic chamber method: trace gas
624 exchange fluxes (NO, NO2, O-3) between plants and the atmosphere in the laboratory and in the field,
625 Atmospheric Measurement Techniques, 5, 955-989, 2012.Brodeur, J. J., Warland, J. S., Staebler, R. M.,
626 and Wagner-Riddle, C.: Technical note: Laboratory evaluation of a tunable diode laser system for eddy
627 covariance measurements of ammonia flux, Agricultural and Forest Meteorology, 149, 385-391, 2009.
628 Carslaw, D. C.: Evidence of an increasing NO2/NOX emissions ratio from road traffic emissions, Atmospheric
629 Environment, 39, 4793-4802, 2005.
630 Corrsin, S., 1975. Limitations of Gradient Transport Models in Random Walks and in Turbulence, in: Frenkiel, F.N.,
631 Munn, R.E. (Eds.), Advances in Geophysics. Elsevier, pp. 25-60.
632 Coyle, M., Nemitz, E., Storeton-West, R., Fowler, D., and Cape, J. N.: Measurements of ozone deposition to a
633 potato canopy, Agricultural and Forest Meteorology, 149, 655-666, 2009.
634 Davidson, E. A.: Sources of Nitric-Oxide and Nitrous-Oxide Following Wetting of Dry Soil, Soil Science
635 Society of America Journal, 56, 95-102, 1992.
636 Davidson, E. A. and Kingerlee, W.: A global inventory of nitric oxide emissions from soils, Nutrient Cycling in
637 Agroecosystems, 48, 37-50, 1997.
638 De Arellano, J. V.-G., Duynkerke, P. G., and Builtjes, P. J. H.: The divergence of the turbulent diffusion flux in
639 the surface layer due to chemical reactions: the NO-O3-NO2 system, Tellus B, 45, 23-33, 1993.
640 Donahue, N. M., Hartz, K. E. H., Chuong, B., Presto, A. A., Stanier, C. O., Rosenhorn, T., Robinson, A. L., and
641 Pandis, S. N.: Critical factors determining the variation in SOA yields from terpene ozonolysis: A
642 combined experimental and computational study, Faraday Discussions, 130, 295-309, 2005.
643 Dubowski, Y., Vieceli, J., Tobias, D. J., Gomez, A., Lin, A., Nizkorodov, S. A., McIntire, T. M., and Finlayson-
644 Pitts, B. J.: Interaction of gas-phase ozone at 296 K with unsaturated self-assembled monolayers: A new
645 look at an old system, Journal of Physical Chemistry A, 108, 10473-10485, 2004.
646 Dunfield, P. F. and Knowles, R.: Nitrogen monoxide production and consumption in an organic soil, Biology
647 and Fertility of Soils, 30, 153-159, 1999.
648 Duyzer, J. H., Deinum, G., and Baak, J.: The Interpretation of Measurements of Surface Exchange of Nitrogen-
649 Oxides - Correction for Chemical-Reactions, Philosophical Transactions of the Royal Society a-
650 Mathematical Physical and Engineering Sciences, 351, 231-248, 1995.
651 EEA: EMEP/EEA air pollutant emission inventory guidebook. Chapter 3D: Crop production and agricultural
652 soils - 2016
653 Eugster, W. and Hesterberg, R.: Transfer resistances of NO2 determined from eddy correlation flux
654 measurements over a litter meadow at a rural site on the Swiss plateau, Atmospheric Environment, 30,
655 1247-1254, 1996.
656 Eugster, W. and Senn, W.: A Cospectral Correction Model for Measurement of Turbulent No2 Flux, Bound-Lay
657 Meteorol, 74, 321-340, 1995.
658 Fares, S., McKay, M., Holzinger, R., and Goldstein, A. H.: Ozone fluxes in a Pinus ponderosa ecosystem are
659 dominated by non-stomatal processes: Evidence from long-term continuous measurements, Agricultural
660 and Forest Meteorology, 150, 420-431, 2010.
661 Feilberg, A., Bildsoe, P., and Nyord, T.: Application of PTR-MS for Measuring Odorant Emissions from Soil
662 Application of Manure Slurry, Sensors, 15, 1148-1167, 2015.
663 Ferrara, R. M., Loubet, B., Di Tommasi, P., Bertolini, T., Magliulo, V., Cellier, P., Eugster, W., and Rana, G.:
664 Eddy covariance measurement of ammonia fluxes: Comparison of high frequency correction
665 methodologies, Agricultural and Forest Meteorology, 158, 30-42, 2012.

Fick, J., Pommer, L., Astrand, A., Ostin, R., Nilsson, C., and Andersson, B.: Ozonolysis of monoterpenes in mechanical ventilation systems, Atmospheric Environment, 39, 6315-6325, 2005.
Foken, T.: The energy balance closure problem: An overview, Ecological Applications, 18, 1351-1367, 2008.
Forster, P., Ramaswamy, V., Artaxo, P., Berntsen, T., Betts, R., Fahey, D. W., Haywood, J., Lean, J., Lowe, D. C., Myhre, G., Nganga, J., Prinn, R., Raga, G., M., S., and Van Dorland, R.: Changes in Atmospheric Constituents and in Radiative Forcing. In: Climate Change 2007: The Physical Science Basis. Contribution of Working Group I to the Fourth Assessment Report of the Intergovernmental Panel on Climate Change Solomon, S., D. Qin, M. Manning, Z. Chen, M. Marquis, K.B. Averyt, M.Tignor and H.L. Miller (eds.) (Ed.), Cambridge University Press, Cambridge, United Kingdom and New York, NY, USA., 2007.
Geddes, J. A. and Murphy, J. G.: Observations of reactive nitrogen oxide fluxes by eddy covariance above two midlatitude North American mixed hardwood forests, Atmos Chem Phys, 14, 2939-2957, 2014.
Gerosa, G., Marzuoli, R., Cieslik, S., and Ballarin-Denti, A.: Stomatal ozone fluxes over a barley field in Italy. "Effective exposure" as a possible link between exposure- and flux-based approaches, Atmospheric Environment, 38, 2421-2432, 2004.
Gerosa, G., Vitale, M., Finco, A., Manes, F., Denti, A. B., and Cieslik, S.: Ozone uptake by an evergreen Mediterranean Forest (Quercus ilex) in Italy. Part I: Micrometeorological flux measurements and flux partitioning, Atmospheric Environment, 39, 3255-3266, 2005.
Godde, M. and Conrad, R.: Influence of soil properties on the turnover of nitric oxide and nitrous oxide by nitrification and denitrification at constant temperature and moisture, Biology and Fertility of Soils, 32, 120-128, 2000.
Gut, A., Blatter, A., Fahrni, M., Lehmann, B. E., Neftel, A., and Staffelbach, T.: A new membrane tube technique (METT) for continuous gas measurements in soils, Plant and Soil, 198, 79-88, 1998.
Gut, A., Neftel, A., Staffelbach, T., Riedo, M., and Lehmann, B. E.: Nitric oxide flux from soil during the growing season of wheat by continuous measurements of the NO soil-atmosphere concentration gradient: A process study, Plant and Soil, 216, 165-180, 1999.
Henault, C., Bizouard, F., Laville, P., Gabrielle, B., Nicoullaud, B., Germon, J. C., and Cellier, P.: Predicting in situ soil N2O emission using NOE algorithm and soil database, Global Change Biology, 11, 115-127, 2005.
Horii, C. V., Munger, J. W., Wofsy, S. C., Zahniser, M., Nelson, D., and McManus, J. B.: Fluxes of nitrogen oxides over a temperate deciduous forest, Journal of Geophysical Research-Atmospheres, 109, 2004.
Horvath, E., Hoffer, A., Sebok, F., Dobolyi, C., Szoboszlay, S., Kriszt, B., and Gelencser, A.: Experimental evidence for direct sesquiterpene emission from soils, Journal of Geophysical Research-Atmospheres, 117, 2012.
Houghton, J. T., Y. Ding, D.J. Griggs, M. Noguer, P.J. van der Linden, X. Dai, K.Maskell, and Johnson, C. A.: IPCC, 2001: Climate Change 2001: The Scientific Basis. Contribution of Working Group I to the Third Assessment Report of the Intergovernmental Panel on Climate Change 881 pp., 2001.
Jammoul, A., Gligorovski, S., George, C., and D'Anna, B.: Photosensitized heterogeneous chemistry of ozone on organic films, Journal of Physical Chemistry A, 112, 1268-1276, 2008.
Kaimal, J. C. and Finnigan, J. J.: Atmospheric Boundary Layer Flows, Their structure and measurement., Oxford University Press., New York, 1994.
Kramm, G., Muller, H., Fowler, D., Hofken, K. D., Meixner, F. X., and Schaller, E.: A Modified Profile Method for Determining the Vertical Fluxes of No, No2, Ozone, and Hno3 in the Atmospheric Surface-Layer, Journal of Atmospheric Chemistry, 13, 265-288, 1991.
Langford, B., Acton, W., Ammann, C., Valach, A., and Nemitz, E.: Eddy-covariance data with low signal-to-noise ratio: time-lag determination, uncertainties and limit of detection, Atmos. Meas. Tech., 8, 4197-4213, 2015.
Laville, P., Flura, D., Gabrielle, B., Loubet, B., Fanucci, O., Rolland, M. N., and Cellier, P.: Characterisation of soil emissions of nitric oxide at field and laboratory scale using high resolution method, Atmospheric Environment, 43, 2648-2658, 2009.
Laville, P., Henault, C., Gabrielle, B., and Serca, D.: Measurement and modelling of NO fluxes on maize and wheat crops during their growing seasons: effect of crop management, Nutrient Cycling in Agroecosystems, 72, 159-171, 2005.
Laville, P., Lehuger, S., Loubet, B., Chaumartin, F., and Cellier, P.: Effect of management, climate and soil conditions on N2O and NO emissions from an arable crop rotation using high temporal resolution measurements, Agricultural and Forest Meteorology, 151, 228-240, 2011.
Lee, J. D., Helfter, C., Purvis, R. M., Beevers, S. D., Carslaw, D. C., Lewis, A. C., Moller, S. J., Tremper, A., Vaughan, A., and Nemitz, E. G.: Measurement of NOx Fluxes from a Tall Tower in Central London, UK and Comparison with Emissions Inventories, Environmental Science & Technology, 49, 1025-1034, 2015.

Lenschow, D. and Delany, A. C.: An analytic formulation for NO and NO2 flux profiles in the atmospheric surface layer, Journal of Atmospheric Chemistry, 5, 301-309, 1987.
Lenschow, D. H., Mann, J., and Kristensen, L.: How Long Is Long Enough When Measuring Fluxes and Other Turbulence Statistics, Journal of Atmospheric and Oceanic Technology, 11, 661-673, 1994.
Lenschow, D. H. and Raupach, M. R.: The Attenuation of Fluctuations in Scalar Concentrations through Sampling Tubes, Journal of Geophysical Research-Atmospheres, 96, 15259-15268, 1991.
Lenschow, D. H., Wulfmeyer, V., and Senff, C.: Measuring second- through fourth-order moments in noisy data, Journal of Atmospheric and Oceanic Technology, 17, 1330-1347, 2000.
Li, J. S., Chen, W., and Fischer, H.: Quantum Cascade Laser Spectrometry Techniques: A New Trend in Atmospheric Chemistry, Applied Spectroscopy Reviews, 48, 523-559, 2013.
Loubet, B., Cellier, P., Flechard, C., Zurfluh, O., Irvine, M., Lamaud, E., Stella, P., Roche, R., Durand, B., Flura, D., Masson, S., Laville, P., Garrigou, D., Personne, E., Chelle, M., and Castell, J.-F.: Investigating discrepancies in heat, CO2 fluxes and O-3 deposition velocity over maize as measured by the eddy-covariance and the aerodynamic gradient methods, Agricultural and Forest Meteorology, 169, 35-50, 2013.
Loubet, B., Genermont, S., Ferrara, R., Bedos, G., Decuq, G., Personne, E., Fanucci, O., Durand, B., Rana, G., and Cellier, P.: An inverse model to estimate ammonia emissions from fields, European Journal of Soil Science, 61, 793-805, 2010.
Loubet, B., Laville, P., Lehuger, S., Larmanou, E., Flechard, C., Mascher, N., Génermont, S., Roche, R., Ferrara, R. M., Stella, P., Personne, E., Durand, B., Decuq, C., Flura, D., Masson, S., Fanucci, O., Rampon, J.-N., Siemens, J., Kindler, R., Schrumpf, M., Gabriele, B., and Cellier, P.: Carbon, nitrogen and Greenhouse gases budgets over a four years crop rotation In northern France, Plant and Soil, 343, 109-137, 2011.
Mahrt, L.: Computing turbulent fluxes near the surface: Needed improvements, Agricultural and Forest Meteorology, 150, 501-509, 2010.
Marr, L. C., Moore, T. O., Klapmeyer, M. E., and Killar, M. B.: Comparison of NOx Fluxes Measured by Eddy Covariance to Emission Inventories and Land Use, Environmental Science & Technology, 47, 1800-1808, 2013.
Martin, R. V., Jacob, D. J., Chance, K., Kurosu, T. P., Palmer, P. I., and Evans, M. J.: Global inventory of nitrogen oxide emissions constrained by space-based observations of NO2 columns, Journal of Geophysical Research-Atmospheres, 108, 2003.
Massman, W. J. and Ibrom, A.: Attenuation of concentration fluctuations of water vapor and other trace gases in turbulent tube flow, Atmos Chem Phys, 8, 6245-6259, 2008.
Mauder, M., Foken, T., Clement, R., Elbers, J. A., Eugster, W., Grunwald, T., Heusinkveld, B., and Kolle, O.: Quality control of CarboEurope flux data - Part 2: Inter-comparison of eddy-covariance software, Biogeosciences, 5, 451-462, 2008.
Mauder, M. and T. Foken.: Impact of post-field data processing on eddy covariance flux estimates and energy balance closure. Meteorologische Zeitschrift, 15: 597-609, 2006.
Meixner, F. X.: The surface exchange of nitric oxide, 1997.
Milford, C., Theobald, M. R., Nemitz, E., Hargreaves, K. J., Horvath, L., Raso, J., Daemmgen, U., Neftel, A., Jones, S. K., Hensen, A., Loubet, B., Cellier, P., and Sutton, M. A.: Ammonia fluxes in relation to cutting and fertilization of an intensively managed grassland derived from an inter-comparison of gradient measurements, Biogeosciences, 6, 819-834, 2009.
Min, K. E., Pusede, S. E., Browne, E. C., LaFranchi, B. W., Wooldridge, P. J., and Cohen, R. C.: Eddy covariance fluxes and vertical concentration gradient measurements of NO and NO2 over a ponderosa pine ecosystem: observational evidence for within-canopy chemical removal of NOx, Atmos Chem Phys, 14, 5495-5512, 2014.
Minoura, H. and Ito, A.: Observation of the primary NO2 and NO oxidation near the trunk road in Tokyo, Atmospheric Environment, 44, 23-29, 2010.
Muller, J. B. A., Percival, C. J., Gallagher, M. W., Fowler, D., Coyle, M., and Nemitz, E.: Sources of uncertainty in eddy covariance ozone flux measurements made by dry chemiluminescence fast response analysers, Atmospheric Measurement Techniques, 3, 163-176, 2010a.
Muller, M., Graus, M., Ruuskanen, T. M., Schnitzhofer, R., Bamberger, I., Kaser, L., Titzmann, T., Hortnagl, L., Wohlfahrt, G., Karl, T., and Hansel, A.: First eddy covariance flux measurements by PTR-TOF, Atmospheric Measurement Techniques, 3, 387-395, 2010b.
Murphy, J. G., Day, D. A., Cleary, P. A., Wooldridge, P. J., Millet, D. B., Goldstein, A. H., and Cohen, R. C.: The weekend effect within and downwind of Sacramento - Part 1: Observations of ozone, nitrogen oxides, and VOC reactivity, Atmos Chem Phys, 7, 5327-5339, 2007.
Nieder, R. and D.K. Benbi: Carbon and Nitrogen in the Terrestrial Environment. Springer, 2008.

Oikawa, P. Y., Ge, C., Wang, J., Eberwein, J. R., Liang, L. L., Allsman, L. A., Grantz, D. A., and Jenerette, G. D.: Unusually high soil nitrogen oxide emissions influence air quality in a high-temperature agricultural region, Nat Commun, 6, 8753, 2015.

Oswald, R., Behrendt, T., Ermel, M., Wu, D., Su, H., Cheng, Y., Breuninger, C., Moravek, A., Mougin, E., Delon, C., Loubet, B., Pommerening-Röser, A., Sörgel, M., Pöschl, U., Hoffmann, T., Andreae, M. O., Meixner, F. X., and Trebs, I.: HONO Emissions from Soil Bacteria as a Major Source of Atmospheric Reactive Nitrogen, Science, 341, 1233-1235, 2013.

Pape, L., Ammann, C., Nyfeler-Brunner, A., Spirig, C., Hens, K., and Meixner, F. X.: An automated dynamic chamber system for surface exchange measurement of non-reactive and reactive trace gases of grassland ecosystems, Biogeosciences, 6, 405-429, 2009.

Park, J. H., Fares, S., Weber, R., and Goldstein, A. H.: Biogenic volatile organic compound emissions during BEARPEX 2009 measured by eddy covariance and flux-gradient similarity methods, Atmos Chem Phys, 14, 231-244, 2014.

Peltola, O., Hensen, A., Helfter, C., Belelli Marchesini, L., Bosveld, F. C., van den Bulk, W. C. M., Elbers, J. A., Haapanala, S., Holst, J., Laurila, T., Lindroth, A., Nemitz, E., Röckmann, T., Vermeulen, A. T., and Mammarella, I.: Evaluating the performance of commonly used gas analysers for methane eddy covariance flux measurements: the InGOS inter-comparison field experiment, Biogeosciences, 11, 3163-3186, 2014.

Penuelas, J., Asensio, D., Tholl, D., Wenke, K., Rosenkranz, M., Piechulla, B., and Schnitzler, J. P.: Biogenic volatile emissions from the soil, Plant Cell and Environment, 37, 1866-1891, 2014.

Personne, E., Loubet, B., Herrmann, B., Mattsson, M., Schjoerring, J. K., Nemitz, E., Sutton, M. A., and Cellier, P.: SURFATM-NH3: a model combining the surface energy balance and bi-directional exchanges of ammonia applied at the field scale, Biogeosciences, 6, 1371-1388, 2009.

Plake, D., Soergel, M., Stella, P., Held, A., and Trebs, I.: Influence of meteorology and anthropogenic pollution on chemical flux divergence of the NO-NO2-O-3 triad above and within a natural grassland canopy, Biogeosciences, 12, 945-959, 2015.

Prüss-Üstün, A., Wolf, J., Corvalán, C., Bos, R., and Neira, M.: Preventing Disease through Healthy Environments: A Global Assessment of the Burden of Disease from Environmental Risks, World Health Organization, Geneva, Switzerland, 2016.

Reeser, D. I., Jammoul, A., Clifford, D., Brigante, M., D'Anna, B., George, C., and Donaldson, D. J.: Photoenhanced Reaction of Ozone with Chlorophyll at the Seawater Surface, Journal of Physical Chemistry C, 113, 2071-2077, 2009.

Remde, A., Slemr, F., and Conrad, R.: Microbial-Production and Uptake of Nitric-Oxide in Soil, Fems Microbiology Ecology, 62, 221-230, 1989.

Rummel, U., Ammann, C., Gut, A., Meixner, F. X., and Andreae, M. O.: Eddy covariance measurements of nitric oxide flux within an Amazonian rain forest, Journal of Geophysical Research-Atmospheres, 107, 2002.

Sintermann, J., Spirig, C., Jordan, A., Kuhn, U., Ammann, C., and Neftel, A.: Eddy covariance flux measurements of ammonia by high temperature chemical ionisation mass spectrometry, Atmospheric Measurement Techniques, 4, 599-616, 2011.

Skiba, U., Drewer, J., Tang, Y. S., van Dijk, N., Helfter, C., Nemitz, E., Famulari, D., Cape, J. N., Jones, S. K., Twigg, M., Pihlatie, M., Vesala, T., Larsen, K. S., Carter, M. S., Ambus, P., Ibrom, A., Beier, C., Hensen, A., Frumau, A., Erisman, J. W., Brueggemann, N., Gasche, R., Butterbach-Bahl, K., Neftel, A., Spirig, C., Horvath, L., Freibauer, A., Cellier, P., Laville, P., Loubet, B., Magliulo, E., Bertolini, T., Seufert, G., Andersson, M., Manca, G., Laurila, T., Aurela, M., Lohila, A., Zechmeister-Boltenstern, S., Kitzler, B., Schaufler, G., Siemens, J., Kindler, R., Flechard, C., and Sutton, M. A.: Biosphere-atmosphere exchange of reactive nitrogen and greenhouse gases at the NitroEurope core flux measurement sites: Measurement strategy and first data sets, Agriculture Ecosystems & Environment, 133, 139-149, 2009.

Springs, M., Wells, J. R., and Morrison, G. C.: Reaction rates of ozone and terpenes adsorbed to model indoor surfaces, Indoor Air, 21, 319-327, 2011.

Stella, P., Kortner, M., Ammann, C., Foken, T., Meixner, F. X., and Trebs, I.: Measurements of nitrogen oxides and ozone fluxes by eddy covariance at a meadow: evidence for an internal leaf resistance to NO2, Biogeosciences, 10, 5997-6017, 2013a.

Stella, P., Loubet, B., Lamaud, E., Laville, P., and Cellier, P.: Ozone deposition onto bare soil: a new parameterisation, Agricultural and Forest Meteorology, 151, 669-681, 2011a.

Stella, P., Loubet, B., Laville, P., Lamaud, E., Cazaunau, M., Laufs, S., Bernard, F., Grosselin, B., Mascher, N., Kurtenbach, R., Mellouki, A., Kleffmann, J., and Cellier, P.: Comparison of methods for the determination of NO-O-3-NO2 fluxes and chemical interactions over a bare soil, Atmospheric Measurement Techniques, 5, 1241-1257, 2012.

Stella, P., Personne, E., Lamaud, E., Loubet, B., Trebs, I., and Cellier, P.: Assessment of the total, stomatal, cuticular, and soil 2 year ozone budgets of an agricultural field with winter wheat and maize crops, Journal of Geophysical Research-Biogeosciences, 118, 1120-1132, 2013b.

Stella, P., Personne, E., Loubet, B., Lamaud, E., Ceschia, E., Bonnefond, J. M., Beziat, P., Keravec, P., Mascher, N., Irvine, M., and Cellier, P.: Predicting and partitioning ozone fluxes to maize crops from sowing to harvest: the Surfatm-O3 model, Biogeosciences, 8, 2869-2886, 2011b.

Stokes, G. Y., Buchbinder, A. M., Gibbs-Davis, J. M., Scheidt, K. A., and Geiger, F. M.: Heterogeneous Ozone Oxidation Reactions of 1-Pentene, Cyclopentene, Cyclohexene, and a Menthenol Derivative Studied by Sum Frequency Generation, Journal of Physical Chemistry A, 112, 11688-11698, 2008.

Toenges-Schuller, N., Stein, O., Rohrer, F., Wahner, A., Richter, A., Burrows, J. P., Beirle, S., Wagner, T., Platt, U., and Elvidge, C. D.: Global distribution pattern of anthropogenic nitrogen oxide emissions: Correlation analysis of satellite measurements and model calculations, Journal of Geophysical Research-Atmospheres, 111, 2006.

Tuzet, A., Perrier, A., Loubet, B., and Cellier, P.: Modelling ozone deposition fluxes: The relative roles of deposition and detoxification processes, Agricultural and Forest Meteorology, 151, 480-492, 2011.

Williams, E. J. and Fehsenfeld, F. C.: Measurement of Soil-Nitrogen Oxide Emissions at 3 North-American Ecosystems, Journal of Geophysical Research-Atmospheres, 96, 1033-1042, 1991.

Wolfe, G. M., Thornton, J. A., McKay, M., and Goldstein, A. H.: Forest-atmosphere exchange of ozone: sensitivity to very reactive biogenic VOC emissions and implications for in-canopy photochemistry, Atmos Chem Phys, 11, 7875-7891, 2011.

Wolfe, G. M., Thornton, J. A., Yatavelli, R. L. N., McKay, M., Goldstein, A. H., LaFranchi, B., Min, K. E., and Cohen, R. C.: Eddy covariance fluxes of acyl peroxy nitrates (PAN, PPN and MPAN) above a Ponderosa pine forest, Atmos Chem Phys, 9, 615-634, 2009.

Yienger, J. J. and Levy, H.: Empirical-Model of Global Soil-Biogenic Nox Emissions, Journal of Geophysical Research-Atmospheres, 100, 11447-11464, 1995.

Zhu, Z. L., Sun, X. M., Zhao, F. H., and Meixner, F. X.: Ozone concentrations, flux and potential effect on yield during wheat growth in the Northwest-Shandong Plain of China, Journal of Environmental Sciences-China, 34, 1-9, 2015.

874

875 **Figures**

876

877

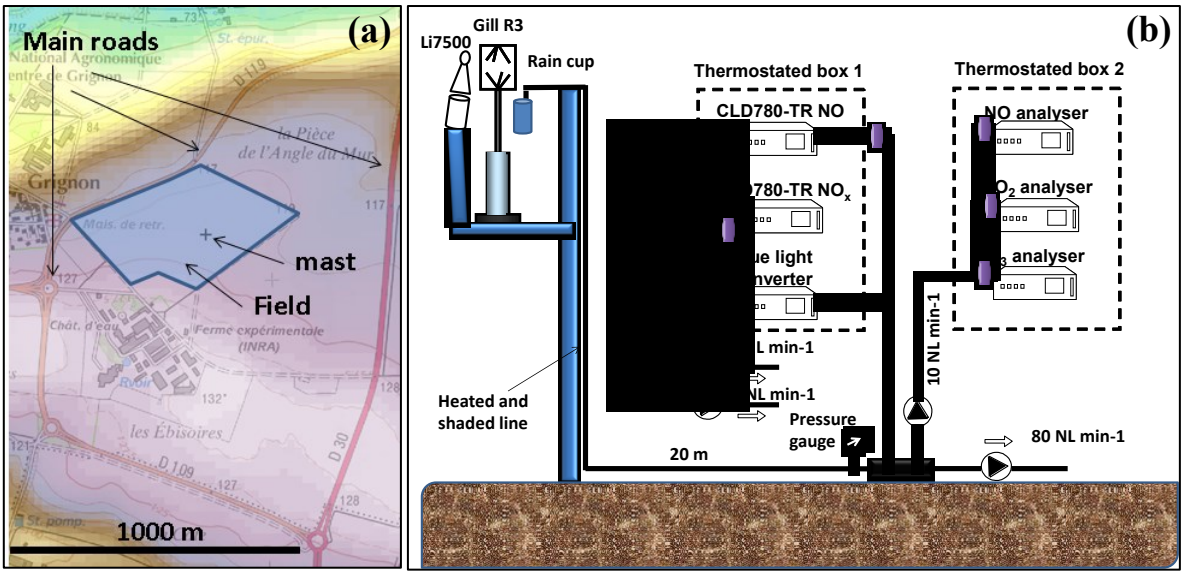

878

879 **Figure 1. (a) Simplified map of the FR-GRI field site showing the mast and surrounding roads. The collors**
880 **correspond to elevation. (b) Simplified sketch of the instrumental setup to measure EC fluxes. Gill R3 is the ultrasonic**
881 **anemometer, Li7500 is the open path infrared CO_2 and H_2O gas analyser, the rain cup is the air sampler for NO and**
882 **NO_2 detection. CLD780-TR NO and NOx are the fast-response NO analysers (Ecophysics) operating in parallel, one**
883 **connected to a BLC measuring NO + αNO_2. The NO, NO_2, and O_3 slow analysers (ThermoScientific, Waltham, USA)**
884 **are placed behind a Teflon pump ensuring atmospheric pressure at the inlet. A large pallet pump ensured a flow rate**
885 **of 80 NL min^{-1} in the heated inlet line. Teflon filters (1µm) were installed at the front of the instrument inlets (purple**
886 **cylinders).**

887

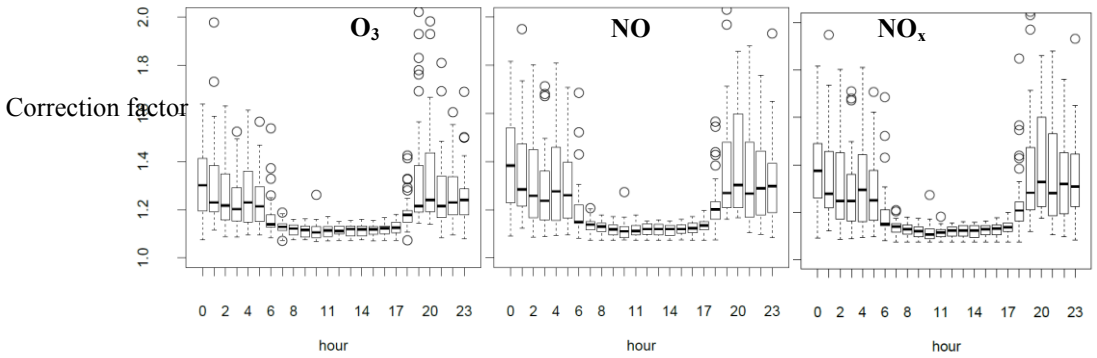

Figure 2. Hourly averaged high frequency loss correction factors for O_3, NO and NO_x over the 15/08/2012 07/09/2012 period determined with the in situ ogive method. The corrected flux equals the measured flux multiplied by the correction factor. Black bars are medians, boxes show the interquartile, error-bars show the minimum and maximum of the whisker and empty dots shows the outliers.

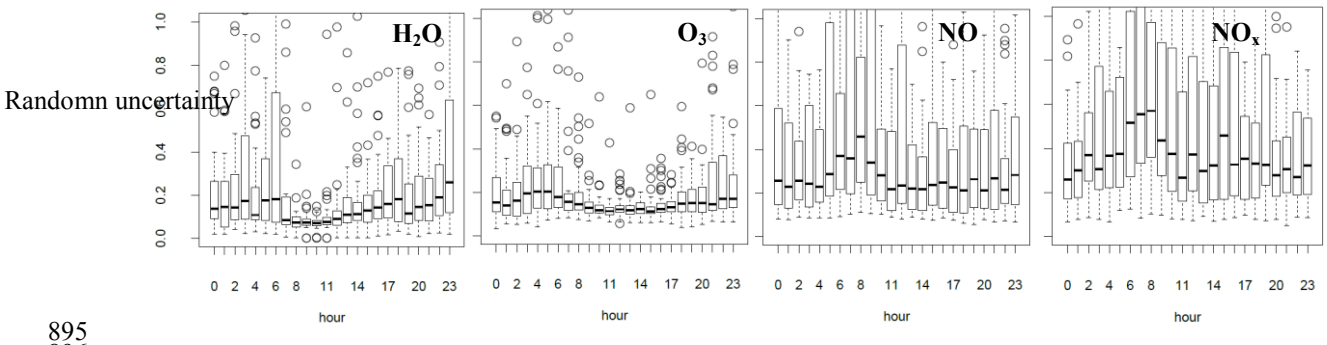

Figure 3. Daily variations of the ratio of the random uncertainty to the flux for H_2O, O_3, NO and NO_x during august 2012 (15/08 to 09/09). Black bars are medians, boxes show the interquartile, error-bars show the minimum and maximum of the whisker and empty dots shows the outliers.

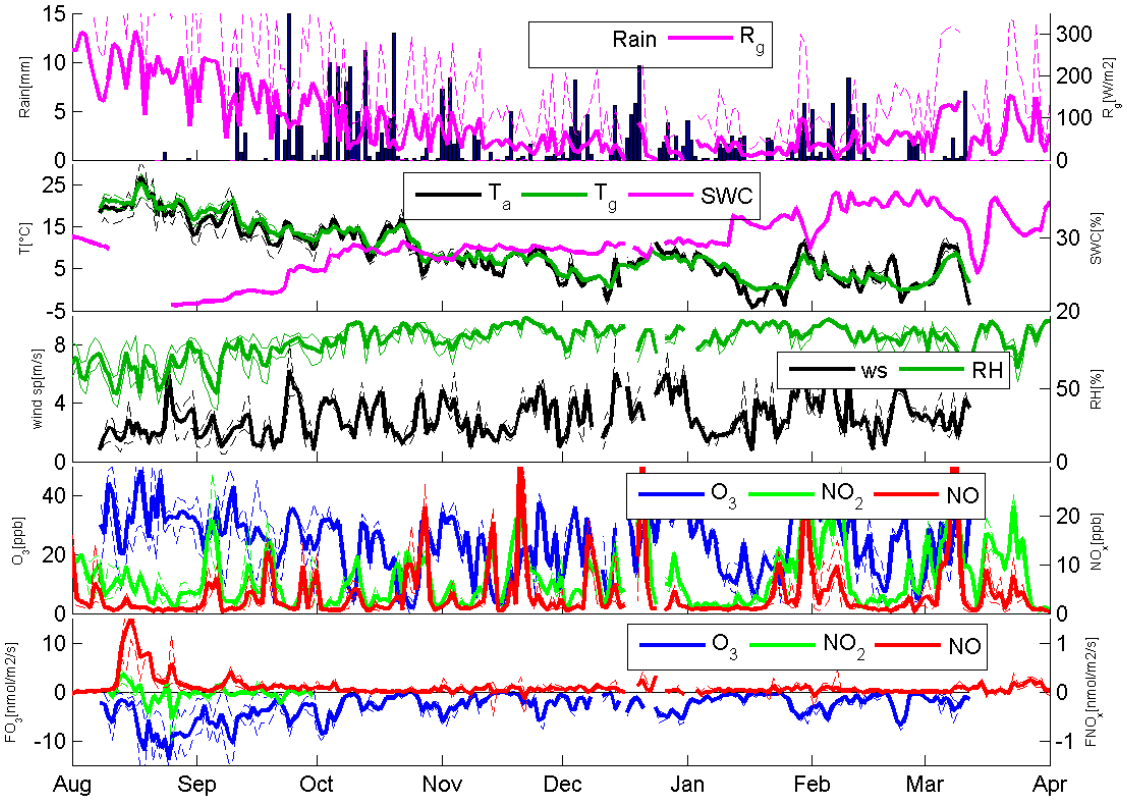

Figure 4. Meteorological and soil conditions (daily averages, sums for rainfall), NO, NO_2 and O_3 mixing ratios and fluxes during the entire measurement period from 07/08/2012 to 13/03/2013 at the Grignon field site. Averages for night-time and daytime are also given as dotted lines. R_g is the global radiation, T_a and T_g the air and ground temperature, SWC the soil water content, ws the wind speed, RH the air relative humidity.

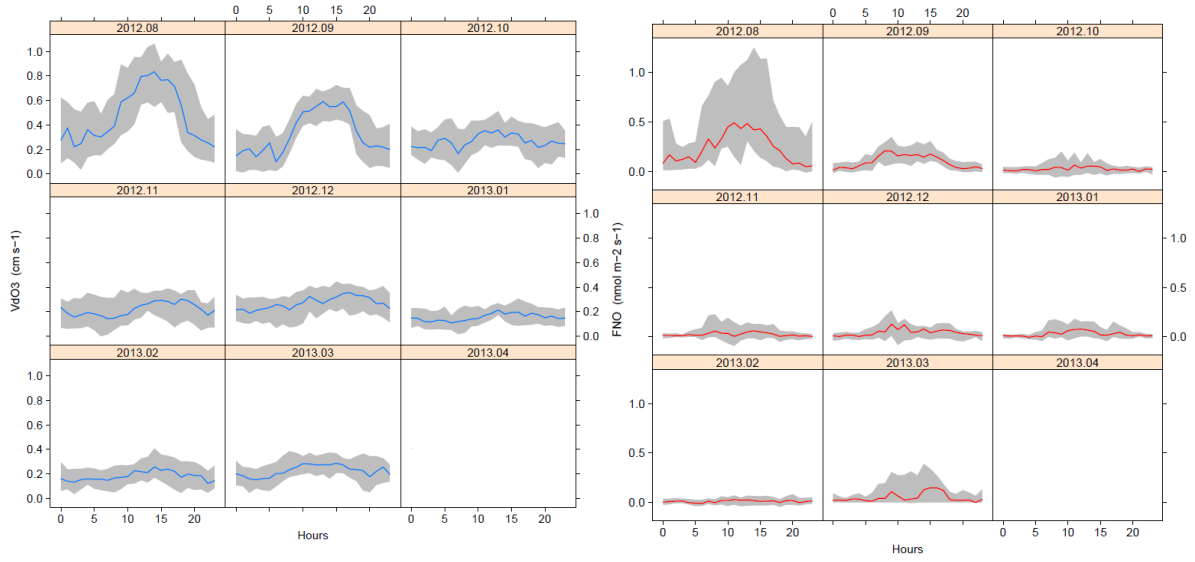

Figure 5. Seasonal changes of ozone deposition velocity VdO3 and NO fluxes. Blue lines show median and grey area inter-quantiles.

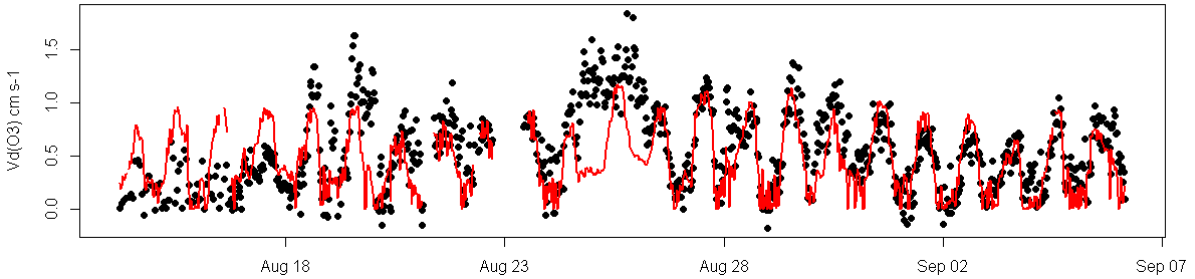

911

912 **Figure 6a. Comparison of ozone deposition velocity from this study (black dots), and from the parameterisation of**
913 **Stella et al. (2011) (red line) based on surface temperature.**

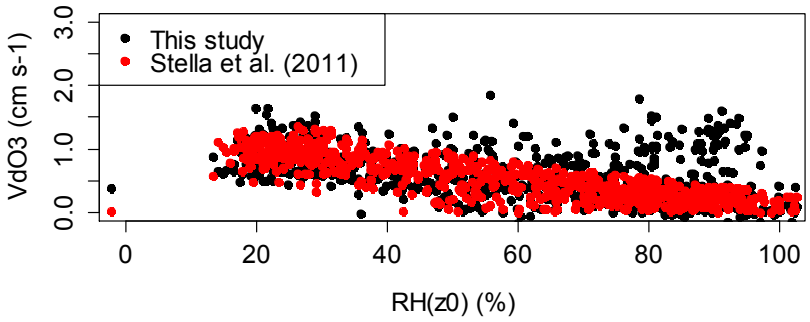

914

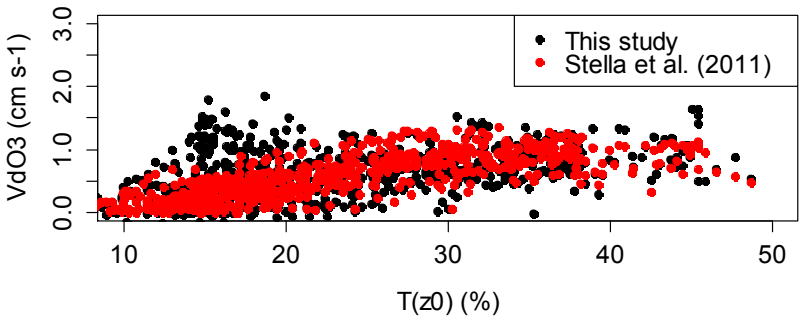

915

916 **Figure 6b. Response of ozone deposition velocity to surface humidity $RH(z_0)$ and surface temperature $T(z_0)$. Shown**
917 **are data from this study and from the parameterisation of Stella et al. (2011). Period from 14 August to 6 September**
918 **which is before and after slurry spreading and corresponds to Figure S5.**

919

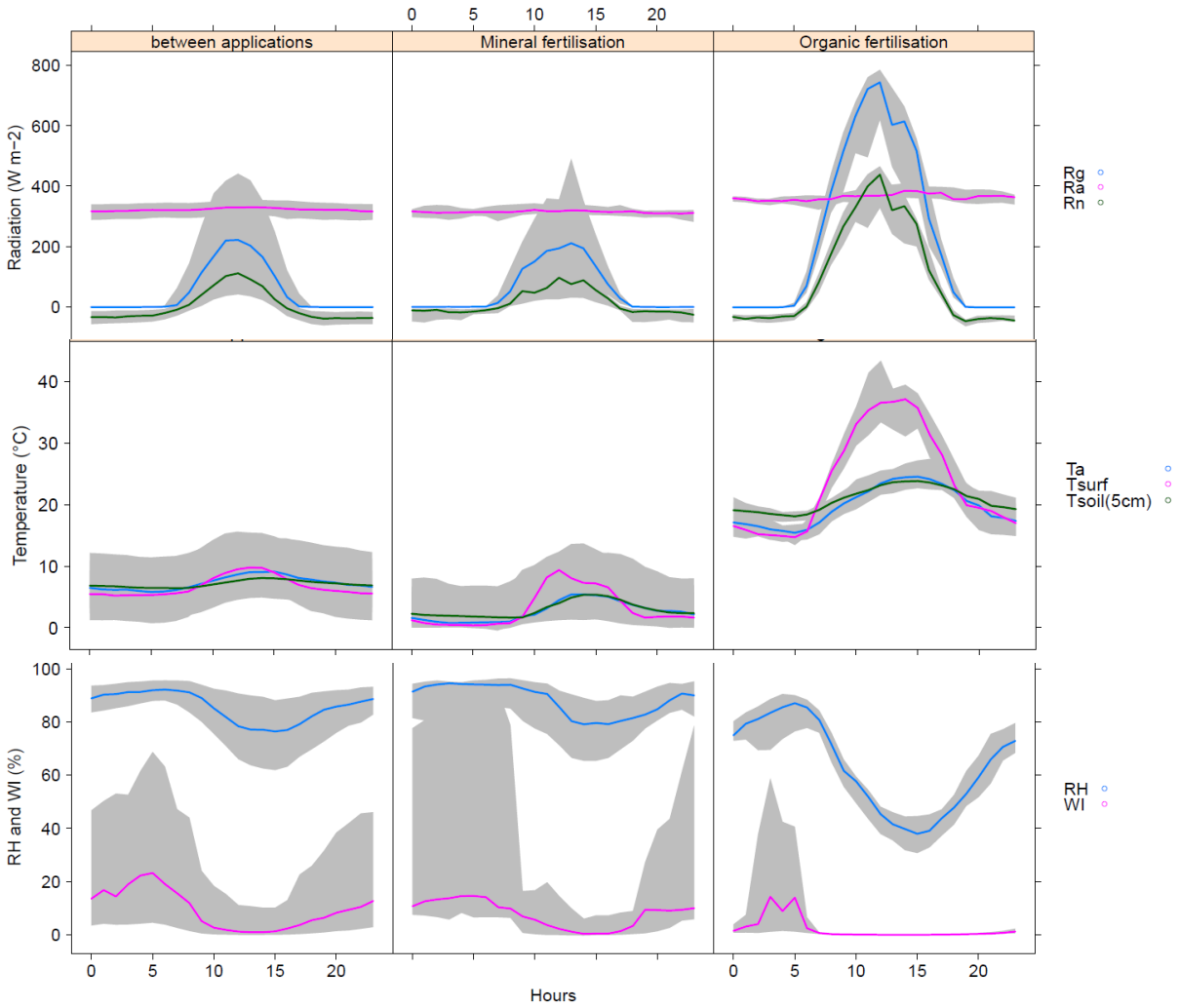

Figure 7a. Diurnal cycles of global irradiance and net radiation, air and soil temperatures, relative humidity and wetness index averaged over the three periods of interest at the Grignon field site. The shaded areas represent the interquartile range.

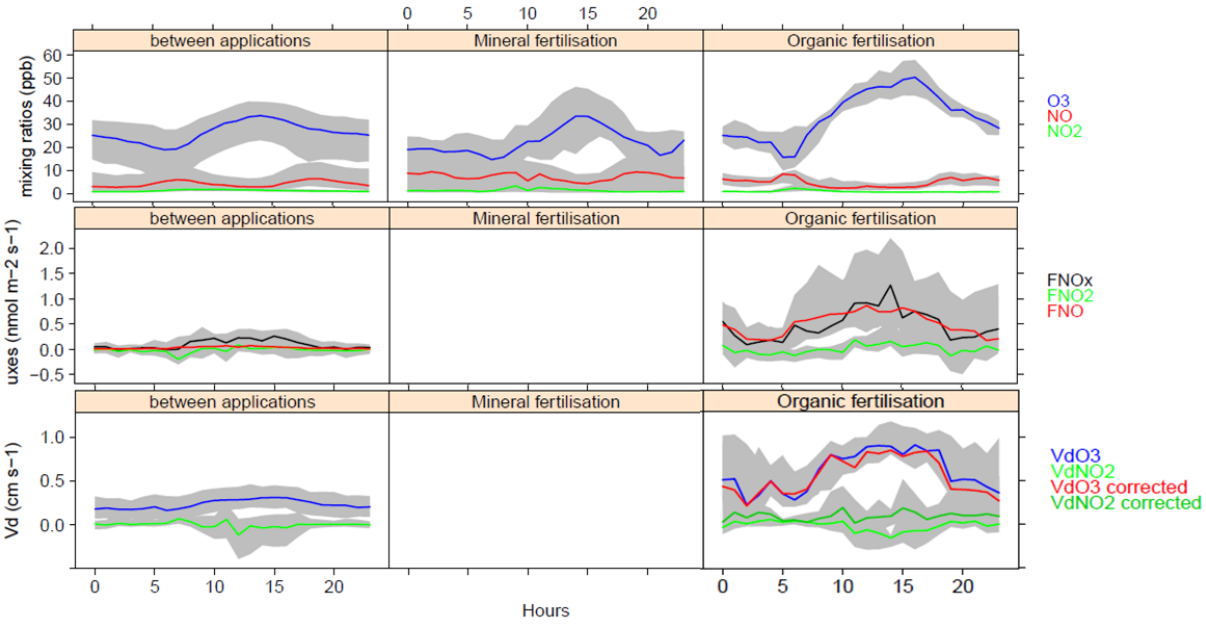

Figure 7b. Diurnal cycles of NO, NO_2 and O_3 mixing ratios and fluxes as well as the deposition velocities of NO_2 and O_3, averaged over the three periods of interest at the Grignon field site. The shaded areas represent the interquartile range. The deposition velocity of NO_2 and O_3 based on the fluxes accounting for chemical reactions above ground are also shown (VdO3 and VdNO2 corrected).

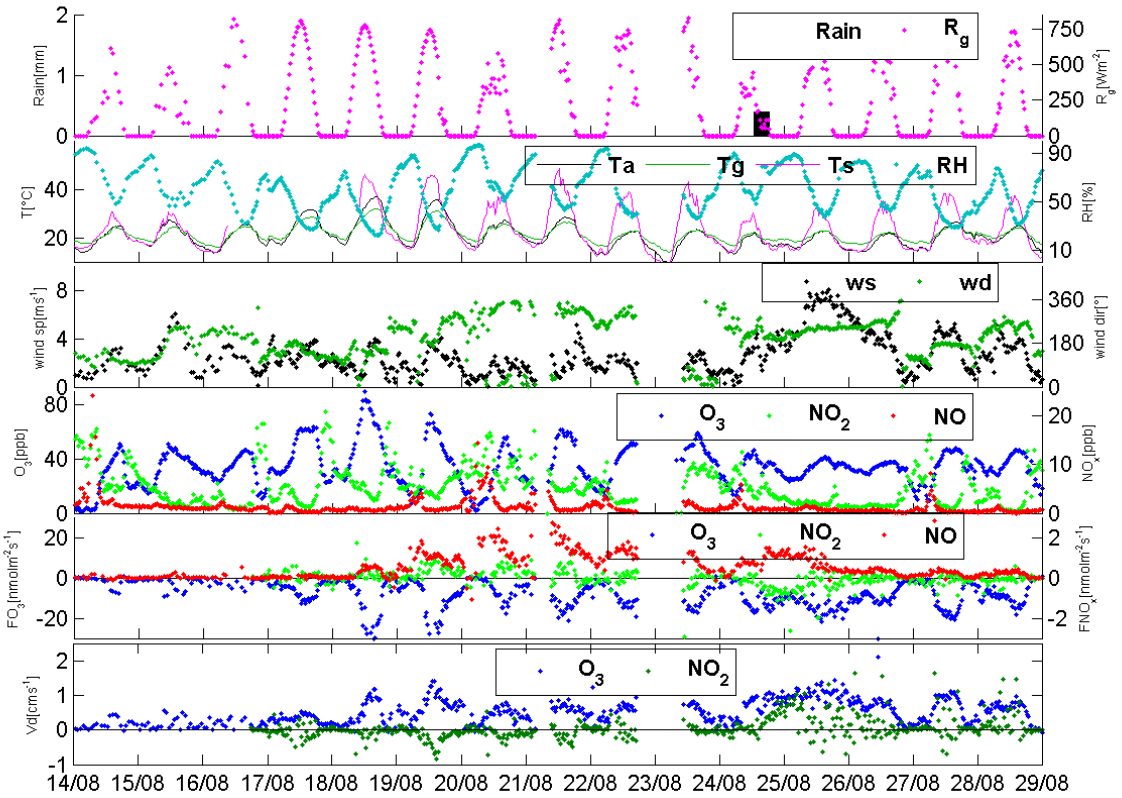

Figure 8. Meteorological variables and NO_x-O_3 mixing ratios and fluxes measured during the period 14/08/12 to 29/08/12 at the Grignon field site. Ticks on the x-axis correspond to midnight.

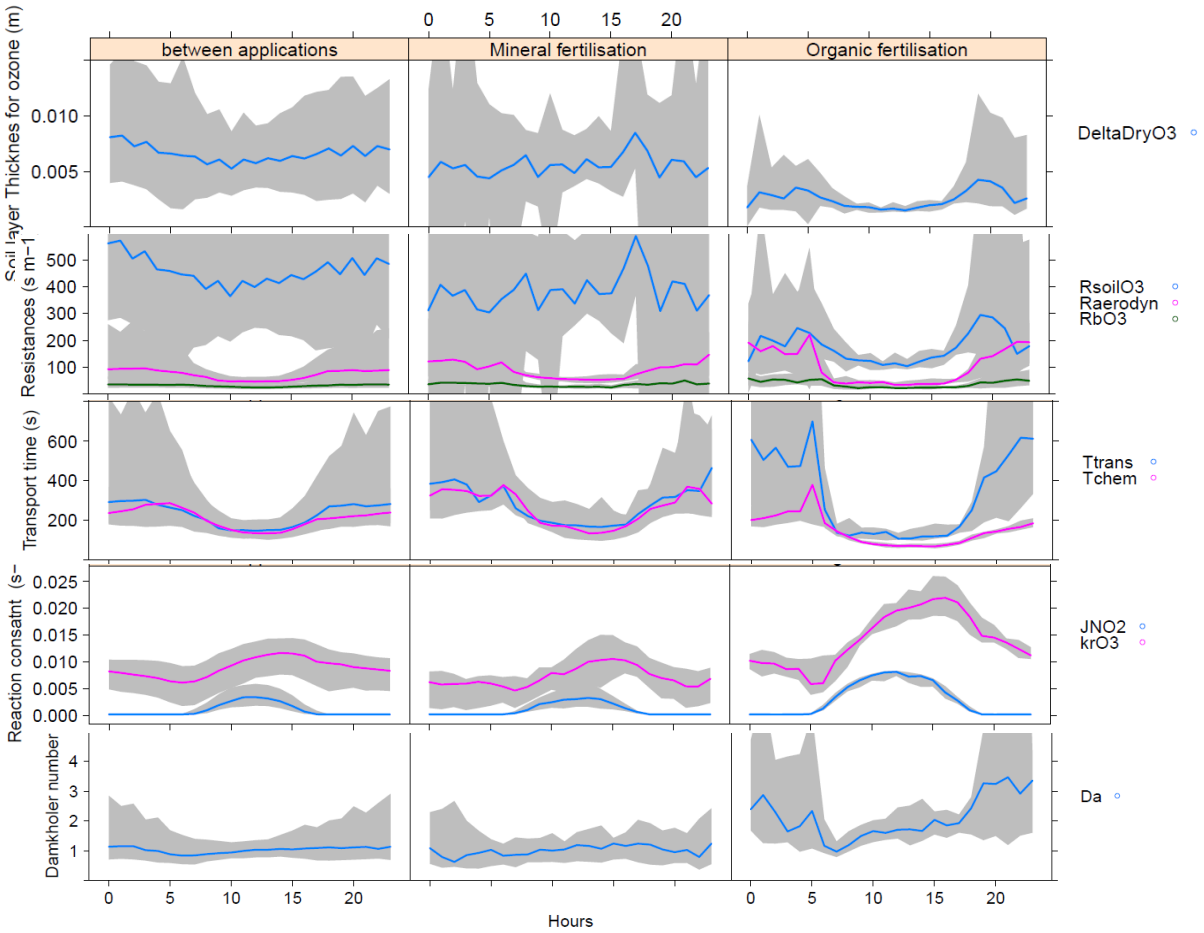

Figure 9. Diurnal cycles of the O_3 penetration depth in the soil (DeltaDryO3), the aerodynamic (Ra), boundary layer (RbO3) and soil resistances (RsoilO3) for O_3, the chemical reaction time τ_{chem} and transport time τ_{trans}, the chemical reaction rates for NO_2 photolysis J_{NO2} and NO depletion by O_3 ($k_r \times [O_3]$), and the Damköhler number (Da), averaged over the periods of interest at the Grignon field site. The shaded areas represent the interquartile range.

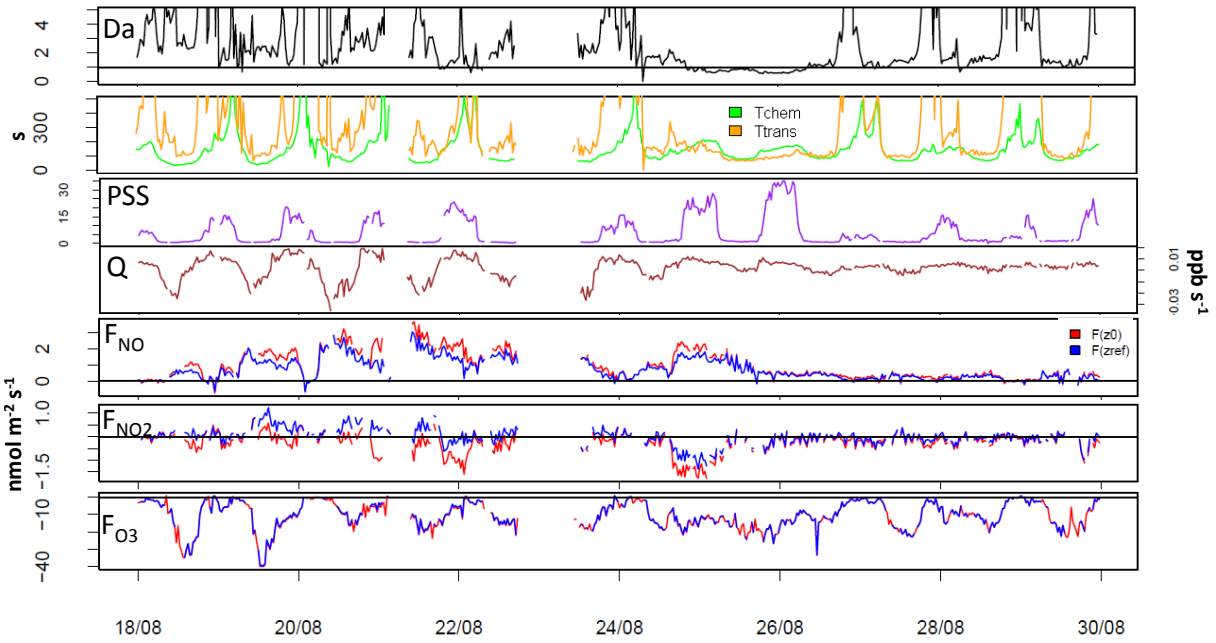

Figure 10. Half-hourly values of photo-stationary state ratio (PSS) and Q = k_r [NO][O_3] - J_{NO2}[NO_2] (s) ; chemistry and transport timescales (Tchem and Ttrans) and Damköhler number (Da); measured NO, NO_2 and O_3 fluxes and surface fluxes as computed by assuming a logarithmic flux divergence profile (F_{NO}, F_{NO2} and F_{O3}) at the Grignon field site.

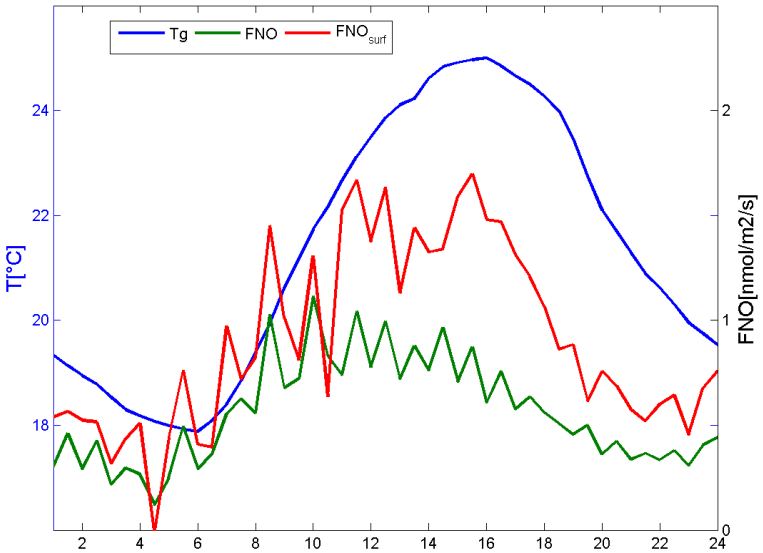

Figure 11. Diurnal cycles of ground temperature, NO flux at measurement height and at surface by the logarithmic profile.